A

Dissertation Report

On

Numerical Simulation of Solar Thermal Energy Conversion System: A CFD Analysis

Submitted in Partial Fulfillment of the Requirements for the Award of Degree of

Master of Technology

In

Thermal Engineering

By

KARAN YADAV

2015PTE5058

Under the supervision of

Dr. M. Mohan Jagadeesh Kumar
Assistant Professor
Department of Mechanical Engineering
M.N.I.T. Jaipur, India

Prof. S. L. Soni
Department of Mechanical Engineering
M.N.I.T. Jaipur, India

DEPARTMENT OF MECHANICAL ENGINEERING

MALAVIYA NATIONAL INSTITUTE OF TECHNOLOGY, JAIPUR

MAY 2017

DEPARTMENT OF MECHANICAL ENGINEERING
JAIPUR (RAJASTHAN)-302017
MALAVIYA NATIONAL INSTITUTE OF TECHNOLOGY

CERTIFICATE

This is certified that the dissertation report entitled **"Numerical simulation of Solar Thermal Energy Conversion system: A CFD Analysis"** prepared by **Karan Yadav** (ID-2015PTE5058), in the partial fulfillment of the award of the Degree **Master of Technology** in **Thermal Engineering** of Malaviya National Institute of Technology, Jaipur is a record of bonafide research work carried out by him under my supervision and is hereby approved for submission. The contents of this dissertation work, in full or in parts, have not been submitted to any other Institute or University for the award of any degree or diploma.

Date:

Place:

Prof. S. L. Soni
Department of Mechanical Engineering
M.N.I.T., Jaipur, India

DEPARTMENT OF MECHANICAL ENGINEERING
MALAVIYA NATIONAL INSTITUTE OF TECHNOLOGY
JAIPUR (RAJASTHAN)-302017

DECLARATION

I **Karan Yadav** hereby declare that the dissertation entitled **"Numerical simulation of Solar Thermal Energy Conversion system: A CFD Analysis"** being submitted by me in partial fulfillment of the degree of **M. Tech (Thermal Engineering)** is a research work carried out by me under the supervision of **Prof. S. L. Soni,** and the contents of this dissertation work, in full or in parts, have not been submitted to any other Institute or University for the award of any degree or diploma. I also certify that no part of this dissertation work has been copied or borrowed from anyone else. In case any type of plagiarism is found out, I will be solely and completely responsible for it.

Date:

Place:

Karan Yadav
M. Tech. (Thermal Engineering)
2015PTE5058

ACKNOWLEDGEMENT

I feel immense pleasure in conveying my heartiest thanks and profound gratitude to my supervisors **Prof. S. L. Soni,** and **Dr. M. Mohan Jagadeesh Kumar** who provided me with their generous guidance, valuable help and endless encouragement by taking personal interest and attention. No words can fully convey my feelings of respect and regard for them.

I would like to express my sincere and profound gratitude to **Mr. Pushpendra Kumar Sharma** (Lab assistant) and all the staff members of the Department of Mechanical Engineering, M.N.I.T., Jaipur, who were abundantly helpful and offered invaluable assistance, support and guidance with their experience and knowledge, throughout my dissertation work.

I also express my deepest gratitude to my **parents**, my **family** and my **friends** for their blessings and affection, without which I would not be able to endure hard time and carry on.

Lastly, but not least I thank one and all who have helped me directly or indirectly in completion of the report.

(Karan Yadav)

ABSTRACT

In recent years, CFD has been attracting much research and development attention from the solar thermal industry because with CFD, effects of various design and operating parameters can be analysed easily and cheaply that cannot be possible with experimental or theoretical studies. Better understanding of the dynamics, underlying physics of the process or phenomenon involved, optimization of existing and new processes can be possible and CFD overcome the need to test the design and develop the actual system with each modification.

Main objective of this study is to develop the CFD model and simulate it with FLUENT to study the different operating parameters of a solar flat plate collector and shell and tube heat exchanger and to optimize its thermal performance.

In this study, detailed literature survey has been carried out and which include the important experimental, theoretical and CFD work carried out by different researchers globally in the field of solar flat plate collector and shell and tube heat exchanger for last two decades.

The geometric modelling was modelled on SOLIDWORKS, meshing (unstructured mesh), defining the types of boundaries of solar flat plate collector and shell and tube heat exchanger and CFD analysis was carried out using FLUENT. For this purpose, a three-dimensional, steady state model of solar flat plate collector and shell tube heat exchanger was developed by employing energy equation with standard k-epsilon turbulence model.

Various important parameters such as mass flow rate of shell side, mass flow rate of tube side, solar radiation, mass flow rate within the collector tubes are optimized to enhance the thermal performance of the solar thermal energy conversion system. Variation in outlet temperature of shell and tube fluid with respect to the variation in mass flow rate of shell and tube side fluid was observed using computational fluid dynamics (CFD) simulations. Increase in solar radiation in solar flat plate collector increases the outlet temperature of fluid and increase in mass flow rate decreases the fluid outlet temperature.

Table of Contents

List of Figures

List of Tables

Nomenclature

m_f	Mass flow rate of fluid (kg/s)
m_{sf}	Mass flow rate of shell fluid (kg/hr)
m_{tf}	Mass flow rate of tube fluid (kg/hr)
ε	Emissivity
ρ	Reflectance
α	Absorbtance
Φ	Inclination angle
τ	Transmittance
ρ	Density (kg/m^3)
K	Thermal Conductivity (W/m.K)
T	Temperature (°C)
C_p	Specific heat (J/kg.K)
U	Overall heat transfer coefficient (W/m^2K)

Nomenclature

CFD	Computational Fluid Dynamics (CFD)
FPC	Flat Plate Collector
ETC	Evacuated Tube Collector
STHX	Shell and tube heat exchanger
LMTD	Log Mean Temperature Difference
CPC	Compound parabolic collector

Chapter 1

Introduction

Environment is facing various adverse effects of depletion of conventional energy sources, and these effects has forced us to drew out attention towards the use of renewable energy resources. So, in order to use renewable energy resources researchers have performed and are performing various research and development activities to identify reliable and economically feasible alternate clean energy sources. Earth has a huge amount of renewable energy resource in its own for example: energy from sun, wave, wind, geothermal, biomass etc. Solar energy is most abundantly available and have high potential to serve human kind with its clean form of energy. Solar energy can be used by various processes like solar PV panel, Solar collector, Solar chimney etc.

There are basically three types of solar thermal collectors: flat plate collector, evacuated tube collector, and concentrating collector. All these collectors have the same purpose of converting the solar energy into heat which can supply the energy demand but there is a lot difference in their geometrical. Heat produced by the solar collectors can be stored or can be use directly to satisfy the energy needs. Thermal performance of the collectors needs to be evaluated in order to match the demand of energy. The instantaneous useful energy collected is the results of an energy balance on the solar collector.

The term flat plate is slightly misleading in sense that surface may not be truly flat – it may be a combination of flat, grooved or of other shapes as the absorbing surface with some kind of heat removal device like tubes or channels.

The glazing covers are used to reduce the convection and radiation heat losses to the environment. When solar radiation travels through the cover then the collector gains energy and both beam and diffuse solar radiation are used during the production of heat. The greater the transmittance (τ) is, the more radiation reaches the absorber plate. Such energy is absorbed in a fraction equal to the absorptivity (α) of the blackened-metal receiver. In general terms, solar collector present great heat losses. Although, the glazing does not allow infrared-thermal energy (long wavelength) to escape, the

temperature difference between the absorber plate and the ambient causes heat losses by convection.

A fluid flows through the passage attached with the absorber plate and gains the heat from absorber surface and thus the fluid temperature increases. This heat energy of the fluid can be used in various applications. Energy gain by the fluid is termed as the useful energy which is the fraction of total energy incident after the heat losses. The instantaneous thermal efficiency corresponds to the amount of energy used from the incoming solar radiation.

1.1 History and Utilisation of Solar Energy

Solar energy can be used in many ways. It can be used as light, heat, and electricity. The diversity in solar energy makes it as an important option to power different energy systems throughout the world. Conventional energy depletion leads us to increase our interest in the use of solar energy system. These efforts of utilization of solar energy can solve the problem of depletion of conventional energy sources and could lead the human life for thousands of years with the clean and pure form of energy.

Solar energy is the most considerable energy source in the world. Sun, has a distance of 1.495×10^{11} (m) from the earth and has a diameter of 1.39×10^{9} (m), and emits approximately 1353 (W/m^2) of solar radiations on a surface perpendicular to rays, if there was no atmospheric layer. The world receives 170 trillion (kW) solar energy and 30% of this energy is reflected back to the space, 47% is transformed to low temperature heat energy, 23% is used for evaporation/rainfall cycle in the Biosphere and less than 0.5% is used in the kinetic energy of the wind, waves and photosynthesis of plants.

Solar energy systems have a very simple concept to utilise the solar energy. Solar collector receives the solar radiations thus the surface temperature increases this increase in temperature leads to heat transfer from absorber plate to the working fluid. Solar collectors are basic part that effect the performance of the system so to increase the performance of the systems, generally modifications performed on solar collectors.

1.2 Overview of Solar Collector

Solar collectors are the key component of active solar-heating systems. They gather the sun's energy, transform its radiation into heat, and then transfer that heat to a fluid (usually water or air). The solar thermal energy can be used in solar water-heating systems, solar pool heaters, and solar space-heating systems.

A solar thermal collector is a device which absorbs the incident solar radiations and converts into heat and further transfer it to the fluid. Solar radiation is energy in the form of electromagnetic radiation from the infrared (long) to the ultraviolet (short) wavelengths.

The term "Solar Collector" commonly refers to solar hot water panels, but may refer to installations such as solar parabolic troughs and solar towers; or basic installations such as solar air heaters. Concentrated solar power plants usually use the more complex collectors to generate electricity by heating a fluid to drive a turbine connected to an electrical generator. Simple collectors are typically used in residential and commercial buildings for space heating. The first solar thermal collector designed for building roofs was patented by **William H. Goettl** and called the "Solar heat collector and radiator for building roof".

There are different types of Solar Collectors which can be used to collect solar incident radiations, the most commonly used are

1. Solar Flat Plate Collector (SFPC)
2. Solar Concentrating Collectors
3. Evacuated Tube Collector (ETC)
4. Parabolic Trough Collector
5. Paraboloid Dish Solar concentrator

Solar collectors are either non-concentrating or concentrating. In the non-concentrating type, the collector area is the same as the absorber area. In these types, the whole solar panel absorbs light. Concentrating collectors have a bigger interceptor than absorber. Flat-plate and evacuated-tube solar collectors are used to collect heat for space heating, domestic hot water or cooling with absorption chillers.

1.3 Solar Flat Plate Collector (SFPC)

Solar energy collectors are special kind of heat exchangers that transform solar radiation energy to internal energy of the transport medium. The major component of any solar system is the solar collector. Of all the solar thermal collectors, the flat plate collectors though produce lower temperatures, have the advantage of being simpler in design, having lower maintenance and lower cost. To obtain maximum amount of solar energy of minimum cost the flat plate solar air heaters with thermal storage have been developed.

A typical flat-plate collector consists of an absorber in an insulated box together with transparent cover sheets (glazing). The absorber is usually made of a metal sheet of high thermal conductivity, such as copper or aluminium, with integrated or attached tubes. The insulated box reduces heat losses from the back and sides of the collector. These Collectors heat liquid or air at temperature less than 80°C.

Flat-plate collectors, developed **by Hottel and Whillier** in the 1950s, are the most common type. They consist of
(1) A dark flat-plate absorber,
(2) A transparent cover that reduces heat losses
(3) A heat-transport fluid (air, antifreeze or water) to remove heat from the absorber,
(4) A heat insulating backing.

The absorber consists of a thin absorber sheet (of thermally stable polymers, aluminium, steel or copper, to which a matte black or selective coating is applied) often backed by a grid or coil of fluid tubing placed in an insulated casing with a glass or polycarbonate cover. In water heat panels, fluid is usually circulated through tubing to transfer heat from the absorber to an insulated water tank. This may be achieved directly or through a heat exchanger.

Fig – 1.1 Solar Flat Plate Collector

Most air heat fabricators and some water heat manufacturers have a completely flooded absorber consisting of two sheets of metal which the fluid passes between. Because the heat exchange area is greater they may be marginally more efficient than traditional absorbers. Sunlight passes through the glazing and strikes the absorber plate, which heats up, changing solar energy into heat energy. The heat is transferred to liquid passing through pipes attached to the absorber plate. Absorber plates are commonly painted with "selective coatings", which absorb and retain heat better than ordinary black paint. Absorber plates are usually made of metal—typically copper or aluminium—because the metal is a good heat conductor. Copper is more expensive, but is a better conductor and less prone to corrosion than aluminium. In locations with average available solar energy, flat plate collectors are sized approximately one half to one square foot per gallon of one day's hot water use.

1.4 Evacuated Tube Collectors

The Evacuated Tube Collector Conductive and convective heat losses are eliminated because there is no air to conduct heat or to cause convective losses. There can still be some radiant heat loss (heat energy will move through a space from a warmer to a cooler surface, even across a vacuum); but this loss is small and of little consequence compared with the amount of heat transferred to the liquid in the absorber tube.

Evacuated tube collectors can be classified in two main groups:

1. Direct flow tubes: the heat transfer fluid flows through the absorber, consists of rows of parallel transparent glass tubes, each of which contains an absorber tube covered with a selective coating.

2. Heat pipe tubes: tubes with heat transfer between the absorber and heat transfer fluid of the collector.

Fig – 1.2 Evacuated Tube Collector

The heat pipe is similar to the direct flow tube type. In this case there is a change of the state of the liquid. Inside the heat pipe there is a small quantity of purified water and some special additives. Due to the vacuum of the tube, the water boils at a lower temperature, typically 30 ºC, so when the heat pipe is heated above 30ºC the water vaporises. This vapour rapidly rises to the top of the heat pipe transferring heat into the condenser. As the heat is lost at the condenser, the vapour condenses to form a liquid and returns to the bottom of the heat pipe and the process starts again.

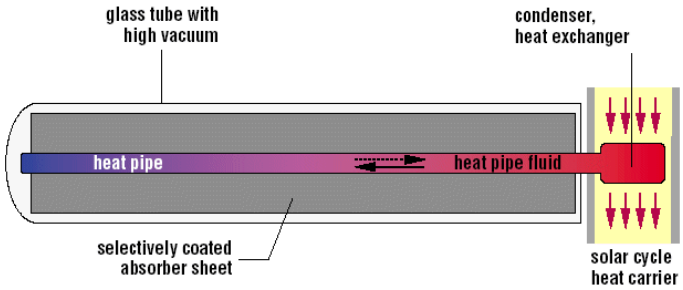

Fig – 1.3 An Evacuated tube collector with heat pipe

1.5 Stationary Concentrating Collectors

Stationary concentrating collectors use compound parabolic reflectors and flat reflectors for directing solar energy to an absorber or aperture through a wide acceptance angle.

The wide acceptance angle for these reflectors eliminates the need for a sun tracker. These collectors are more useful as linear or trough-type concentrators. The acceptance angle is defined as the angles through which a source of light can be moved and still connect at the absorber.

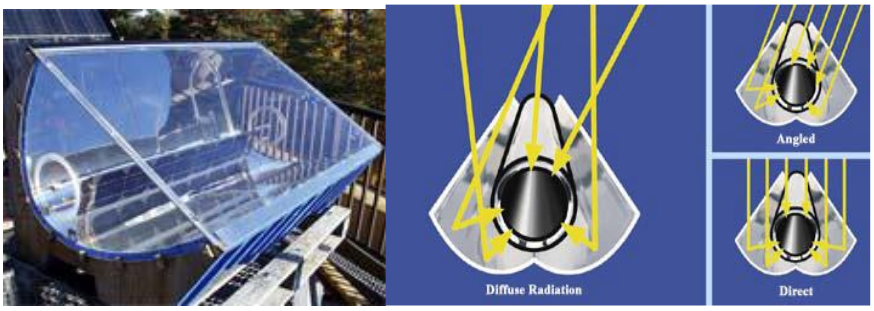

Fig – 1.4 Stationary Concentrating Collector

1.6 Concentrating Solar Collector

Concentrating solar collectors are used when higher temperatures are required. Solar energy which is falling onto a large reflective surface is reflected onto a much smaller area before it is converted into heat. Most concentrating collectors can only concentrate the parallel radiations coming directly from the sun's beam and hence must track the sun's direction across the sky. Three types of solar concentrators are in common use;

1 Central receivers,

2 Parabolic dishes, and

3 Parabolic troughs.

1.6.1 Central Receiver System

A central receiver system illustrated consists of a large field of independently movable flat mirrors (heliostats) and a receiver located at the top of a tower. Each heliostat moves about two axes throughout the day to keep the sun's rays reflected onto the receiver at the top of the tower. The amount of energy coming out of the sun rays when concentrated at one point (the tower in the middle) produces a range of temperatures between 550°C to 1500°C. This thermal energy can be used for heating water or molten salt, which saves the energy for a later use. The water changes to steam which is used to move the turbine-generator; hence thermal energy is converted into electricity.

Fig – 1.5 Central Receiver System

1.6.2 Parabolic Dish

A parabolic dish is a combination of a satellite-dish, a receiver and a Stirling Engine. It concentrates the incoming solar radiation to a point and generates electricity in the range of 5 kW to 25 kW; therefore, it's used as a standalone generator. Solar Dishes use a parabolic mirror to concentrate solar energy at its focal point. Then a receiver, mounted at the focal point, converts the energy of the sun's rays into heat. The heat gained produces a temperature of between 650 ºC to 800 ºC and this is used to drive a Stirling Engine that generates electricity.

Fig – 1.6 Parabolic Dish

1.6.3 Parabolic Trough Collectors

A parabolic trough collector has a linear parabolic-shaped reflector that focuses the sun's radiation onto a linear receiver tube located along the trough's focal line. The collector tracks the sun along one axis from east to west during the day to ensure that the sun is continuously focused on the receiver.

Mechanical drives slowly rotate the troughs during the day to keep the reflected sunlight focused onto the pipe receivers. The fluid flowing in the tube is heated in the range of 300 °C to 400 °C. The working fluid is heated as it circulates through the receivers and returns to a series of heat exchangers at a central location where the fluid is used to generate high-pressure superheated steam. The steam is then fed to a conventional steam turbine/generator to produce electricity. The solar trough generators operating today have gas-fired backup heaters so electricity can be generated during cloudy periods or at night.

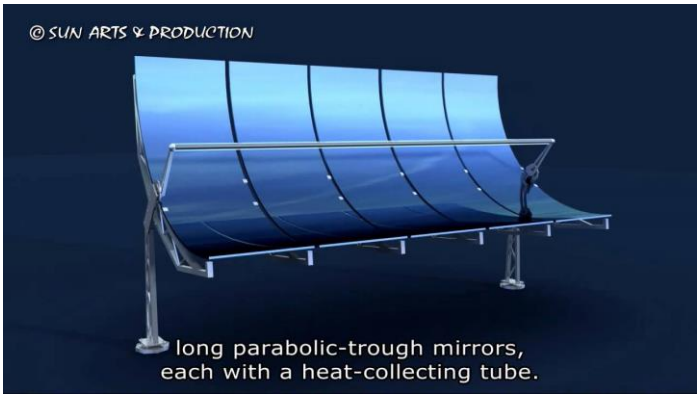

Fig – 1.7 Parabolic Trough Collector

1.7 Shell and Tube Heat Exchanger

Heat exchanger is a device which is used to transfer heat between two fluids. The two fluids can be liquid or gas. Shell and tube heat exchanger is the most widely used heat exchanger because of its unique shape and ability to work under high pressure drop. It is the most common type of heat exchanger in oil refineries and other large chemical processes, and is suited for higher-pressure applications. As its name implies, this type of heat exchanger consists of a shell (a large pressure vessel) with a bundle of tubes inside it. One fluid flows through the tubes, and another over the tubes (through the shell) to transfer heat between the two fluids. The set of tubes is called a tube bundle, and may arranged in several ways: square, triangle, inclined square etc.

Shell and tube heat exchangers are most commonly used heat exchangers in various industrial and research applications. Shell and tube heat exchanger found their importance in high pressure applications because of its unique shape. These heat exchangers can be used for various applications such as heating, cooling, condensation and boiling. In shell and tube heat exchanger generally hot fluid is taken in shell side

and tubes are filled with cold fluid, heat transfer takes place between hot and cold fluid largely through convection. To enhance the heat transfer in a shell and tube heat exchangers various methods can be used. Generally, baffles are used to increase the fluid velocity and heat transfer coefficient which ultimately increases heat transfer through the heat exchanger.

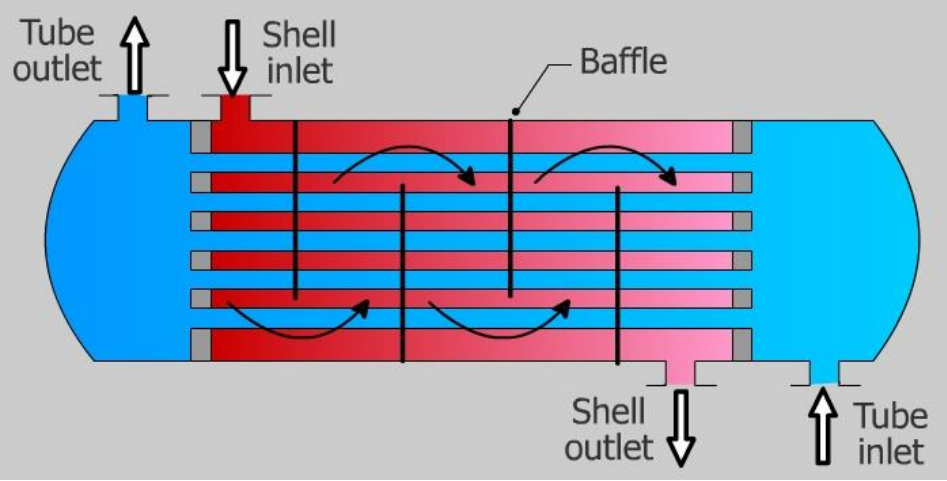

Fig – 1.8 Shell and tube heat exchanger.

The simple design of a shell and tube heat exchanger makes it an ideal for cooling of a wide variety of applications. Most commonly used applications are the cooling of hydraulic fluids and oil in internal combustion engines, transmissions and hydraulic power machines. Shell and tube heat exchangers can also be used to cool or heat other mediums like charged air, swimming pool, thermal storage systems etc. but needs to be care of the right choice of materials, they can also be used to cool or heat other mediums, such as swimming pool water or charge air. One of the big advantages of using a shell and tube heat exchanger is that they are often easy to service, particularly with models where a floating tube bundle (where the tube plates are not welded to the outer shell) is available.

1.8 Importance and Application of CFD technique

In recent years, CFD has been attracting much R&D attention from the solar thermal industry because CFD offers a powerful design and analysis tool to the solar thermal engineer. With CFD, the significance and effects of various design and operating parameters can be analysed that cannot be possible with experimental or theoretical studies. So that better understanding of the dynamics, underlying physics of a process

or phenomenon, optimization of existing and new process can be possible and CFD overcome the need to test the design with each modification.

In the solar thermal industry, many applications involve fluid flow and heat and mass transfer. CFD is currently gaining popularity in many of these areas as it provides an ideal tool for obtaining a qualitative and quantitative assessment of the performance of these facilities.

Therefore, the application of CFD will greatly benefit the solar thermal industry in its frequent chase for process and product improvement. In the present work, an attempt has been made to apply CFD technique for the detailed analysis of solar thermal energy conversion system. Attempts are made to investigate the performance of solar flat plate collector and shell and tube heat exchanger considering the effect of various operating and design parameters.

1.9 Objective of study

To study the thermal performance of solar thermal energy conversion system and optimize its operating parameters. CFD analysis is important apart from the existing method of experimentation and theoretical analysis. Following are the objectives of the study:

i. To study the available work on solar thermal energy conversion system from literature.
ii. To learn simulation software FLUENT 15.0 and SOLIDWORKS 15.0.
iii. Identification of the important parameters and processes involved.
iv. Geometrical modelling of the solar flat plate collector and shell and tube heat exchanger using SOLIDWORKS software.
v. Development of CFD model with FLUENT and analyse considering the simultaneous effect of mass flow rate, heat transfer.
vi. To study the effect of different operating parameters on the performance of solar flat plate collector and shell and tube heat exchanger.
vii. To compare and validate the CFD results with the experimental results and results obtained from other similar studies on the solar flat plate collector and shell and tube heat exchanger.

viii. To draw important conclusion and propose the recommendations for the utilization of the results.

1.10 Outline of thesis

For the convenience in the presentation the thesis has been divided into six chapters. The chapter plan for thesis is as under:

Chapter 1: Introduction

Frist chapter states the introduction and principal of the solar flat plate collector and shell and tube heat exchanger, and objectives of the present study are also included.

Chapter 2: Literature review

In this chapter overviews of the available literatures corresponding to the solar flat plate collector and shell and tube heat exchanger (at world and Indian level) have been discussed. Observations are given for using this knowledge in the present study.

Chapter 3: CFD simulation modelling of solar thermal energy conversion system

This chapter describes about the CFD simulation modelling of solar flat plate collector and shell and tube heat exchanger, problem solving steps in CFD, CFD model development for SFPC and STHX and validation of CFD results.

Chapter 4: Performance analysis of solar thermal energy conversion system with CFD

This chapter illustrates about the effect of mass flow rate and effect of solar radiations on the performance of solar flat plate collector and effect of shell fluid mass flow rate and tube fluid mass flow rate variation on the performance of shell and tube heat exchanger.

Chapter 5: Results and discussion

The results are summarized and discussed in this chapter. A comparative analysis has been made in the form of tables and the obtained results have been discussed. Optimised solar thermal energy conversion system specifications have been discussed in this chapter.

Chapter 6: Conclusions

The important conclusions are summarised in this chapter. Furthermore, possible future developments are suggested and scope of future work is indicated.

Chapter 2

Literature Review

2.1 Solar flat plate collector

Various research studies have been performed to analyse the performance of solar flat plate collector and to improve their performance in order to achieve maximum utilization of solar energy. This chapter overviews some of the latest researches carried out in recent times in the field of solar flat plate collector.

Kalogirou et al. (2004) presents a survey of the various types of solar thermal collectors and applications. All the solar systems which utilize the solar energy and its application depends upon the solar collector such as flat-plate, compound parabolic, evacuated tube, parabolic trough, Fresnel lens, parabolic dish and heliostat field collectors which are used in these systems. The application of solar collector includes solar water heating, which comprise thermo-siphon, integrated collector storage, direct and indirect systems and air systems, space heating and cooling, which comprise, space heating and service hot water, air and water systems and heat pumps, refrigeration, industrial process heat, which comprise air and water systems and steam generation systems, desalination, thermal power systems, which comprise the parabolic trough, power tower and dish systems, solar furnaces, and chemistry applications.

Table-2.1: Comparison of the various Solar Collectors

Motion	Collector Type	Absorber Type	Concentration ratio	Temperature range (°C)
Stationary	FPC	Flat	1	30-80
	ETC	Flat	1	50-200
	CPC	Tubular	1-5	60-240
Single-axis tracking	LFR	Tubular	15-45	60-250
	PTC	Tubular	15-45	60-300
	CTC	Tubular	10-50	60-300
Two-axes tracking	PDR	Point	100-1000	100-500
	HFC	Point	100-1500	150-2000

Prasad et al. (2010) presented experiment analysis of flat plate collector and comparison of performance with tracking collector. A flat plate water heater, which is commercially available with a capacity of 100 litres/day is instrumented and developed into a test-rig to conduct the experimental work. Experiments were conducted for a week during which the atmospheric conditions were almost uniform and data was collected both for fixed and tracked conditions of the flat plate collector. The results show that there is an average increase of 40°C in the outlet temperature. The efficiency of both the conditions was calculated and the comparison shows that there is an increase of about 21% in the percentage of efficiency.

Herrero et al. (2011) describe enhancement techniques for flat-plate liquid solar collectors. Tube-side enhancement passive techniques can consist of adding additional devices which are incorporated into a smooth round tube (twisted tapes, wire coils), modifying the surface of a smooth tube (corrugated and dimpled tubes) or making special tube geometries (internally finned tubes). For the typical operating flow rates in flat-plate solar collectors, the most suitable technique is inserted devices. Based on previous studies from the authors, wire coils were selected for enhancing heat transfer. This type of inserted device provides better results in laminar, transitional and low turbulence fluid flow regimes.

Bakhtiari et al. (2012) performed an experimental analysis of solar flat plate air collector efficiency. Absorber of the flat plate collector having are 2×1 m^2 and thickness of 0.5 mm had been developed in the form of window shade in order to increase the aperture area. Experimental analysis was carried out for a week to analyse the efficiency of collector with natural and force convection flow. It can be concluded from results that collector with natural convection possess better efficiency compared with forced convection. Average efficiency of collector with natural and forced convection was 45.18% and 19.46% respectively.

Ranjitha et al. (2013) performed a numerical simulation for the analysis of solar flat plate collector with circular pipe configurations. In this analysis, experimental and theoretical work was investigated for flow and temperature distribution results and these results were compared with the results of numerical simulation. CFD results were

validated with experimental results and the analysis shows a good agreement between experimental and CFD results with only 5% deviation in outlet temperature.

S. Ramasamy et al. (2015) paper summarizes the previous works on solar water heating systems with various heat transfer enhancement techniques include collector design, collector tilt angle, coating of pipes, fluid flow rate, thermal insulation, integrated collector storage, thermal energy storage, use of phase change materials, and insertion of twisted tapes. This paper also discussed the methods to optimize and simulate the solar water heating systems to understand flow and thermal behaviour in solar collectors that would lead to the improvement of the thermal performance of solar collectors. The enhancement of heat transfer in the solar collector with twisted tape is found to be better than the conventional plain tube collector. In solar water heating systems twisted tape has been used as one of the passive techniques to augment the heat transfer. Twisted tape has been used in heat exchangers but their applications are limited in solar water heating systems.

Krisztina Uzuneanu et al. (2016) describe optimum tilt angle for solar collectors with low concentration ratio. The performance of any solar energy system depends very much on the availability of solar radiation and the orientation of solar collectors. Solar collectors need to be inclined at the optimum angle to maximize the receiving energy. In this work, we proposed to analyse the optimum tilt angle for compound parabolic collectors CPC with different concentration ratios. There are analysed the energy gains when the collector keeps the same position during the whole year and when the collector changes its tilt twice a year, on summer and on winter.

Table-2.2: The optimum tilt angles for different concentration ratio, for summer and winter.

Concentration Ratio (C)	Tilt Angle (β)	Q (kWh/m^2) Useful Energy gain	Tilt Angle (β)	Q (kWh/m^2) Useful Energy gain	Q (kWh/m^2) Useful Energy gain
	Summer		Winter		Year
1	Φ-23	89.065	Φ+2	11.91	97.975
1.2	Φ-23	84.258	Φ+2	12.668	96.926
1.5	Φ-23	85.747	Φ+3	14.435	100.182
1.7	Φ-23	87.035	Φ+4	15.686	102.721
2	Φ-23	89.248	Φ+5	17.419	106.667
2.5	Φ-25	91.248	Φ+4	19.771	111.019
3	Φ-21	92.923	Φ+8	21.376	114.299
3.5	Φ-18	91.658	Φ+10	22.522	114.18
4	Φ-16	89.088	Φ+13	23.396	112.484
4.5	Φ-22	78.928	Φ+15	24.089	103.017
5	Φ-21	77.676	Φ+13	24.20	101.876

2.2 Shell and Tube heat exchanger

Research on shell and tube heat exchangers has been carried out by many researches owing to their applications in all the thermal heat transfer units. Theoretical as well as experimental analysis of shell and tube heat exchangers had been carried out to enhance their performance. Many techniques including addition of baffles, internal and external finned tubes, nano fluids etc., were successfully implemented to improve both internal and external heat transfer coefficients in shell and tube heat exchangers. This chapter presents an overview of the literature on theoretical and experimental analysis of shell and tube heat exchanger carried out by various researchers.

2.2.1 Experimental Review

Experimental works considering various heat exchanger designs had been carried out to find the effect of finned tubes, different baffles, mass flow rate of shell and tube fluids etc., on the performance of shell and tube heat exchangers.

Li et al. (1997) performed an experimental study to analyse the effect of baffle spacing on pressure drop and local heat transfer coefficients in shell and tube heat exchangers with staggered tube arrangement. The distributions of the local heat transfer coefficients on each tube surface within a fully developed baffle compartment were determined and visualised by means of mass transfer measurement. Baffles with three different spacing of 113 mm, 144 mm and 175 mm were considered for the experimental analysis. Per-tube, per-row and per-compartment average heat transfer coefficients were drawn from the local values. Shell-side fluid flow distributions were determined using the local pressure measurements. From the results, it concluded that Nusselt number and Reynolds number increases with the increase in baffles spacing. The pressure drop and average heat transfer for a constant Reynolds number were increased with increased baffle spacing, due to a reduced leakage through the baffle-shell clearance.

Shokouhmand et al. (2007) investigated the performance of shell and coiled tube heat exchanger using Wilson plots. Three heat exchangers with different coil pitches and curvature ratios were tested for both parallel and counter flow configurations. Two coiled tubes with quite similar coil pitches and different curvatures were constructed and tested to study the effect of coiled tube curvature ratio on the heat transfer coefficient. Overall heat transfer coefficients of the heat exchanger were calculated using Wilson plots. It was found from the experimental results that the shell-side heat transfer coefficient will increase with increase in pitches of the coils. It was seen that the shell-side Nusselt numbers of counter-flow configuration were slightly more than that of parallel-flow configuration. It was observed that the overall heat transfer coefficients of counter-flow configuration were 0 to 40 % higher than those of parallel-flow configuration.

Wang et al. (2007) performed an experimental study on shell and tube heat exchanger with continuous helical baffles. In this study, two heat exchangers having same continuous baffles and different shell configurations were designed and tested in which cold water flowed in the tube side and hot oil flowed in the shell side of the heat exchangers. Heat was transferred from hot oil to cold water, and the heat from the cold water was carried away by the cooling water. Heat transfer coefficient per unit pressure drop in the heat exchanger was significantly increased due to the continuous helical baffles. The results indicate that the use of continuous helical baffles results in nearly

10% increase in heat transfer coefficient compared with that of conventional segmental baffles for the same shell side pressure drop. The results indicate that in the low overall pressure drop region, the heat transfer coefficient increases significantly with the increase in the overall pressure drop, while in the high pressure drop region, this increase becomes smaller.

Wang et al. (2008) performed an experimental investigation to enhance the heat transfer in a shell and tube heat exchanger. Sealers were used in the shell side to enhance heat transfer in the shell and tube heat exchanger. The short-circuit flow in the shell-side found to be effectively decreased by blocking the gaps between the baffle plates and shell by using sealers (Fig. 2) as compared to conventional heat exchanger without sealers (Fig. 1). The experimental results show that the shell-side heat transfer coefficient increased by 18.2–25.5%, the overall heat transfer coefficient increased by 15.6–19.7% and the exergy efficiency increased by 12.9–14.1% by blocking the short-circuit flow with sealers. Pressure losses increased by 44.6–48.8% with the sealer installation, but the increment of required pump power can be neglected compared with the increment of heat flux. The heat transfer performance of the improved heat exchanger is intensified, which is an obvious benefit to optimize the heat exchanger design for energy conservation.

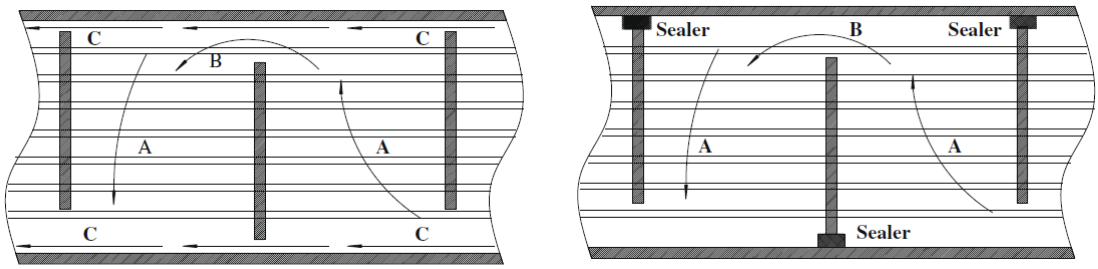

(a) conventional heat exchanger. **(b) improved heat exchanger.**

Fig. 2.1 Schematic flow distribution for baffled shell-side flow

Wang et al. (2011) performed an experimental investigation of a shell and tube heat exchanger with flower baffles (Fig.3) and segmental baffles to compare their performance. The results suggest that under the same working conditions, the overall performance of the heat exchanger with flower baffles is 20–30% more efficient than that of the heat exchanger with segmental baffles. The experimental results showed that

for same Reynolds number both in shell and tube side, the Nusselt number for STHX with flower baffle is about 50% higher than that of STHX with segmental baffles. The pressure drop of the STHX with flower baffles is about 30% higher than that of STHX with segmental baffles, but the comprehensive performance (Nu/Δp) of the former is 60% higher than that of the latter.

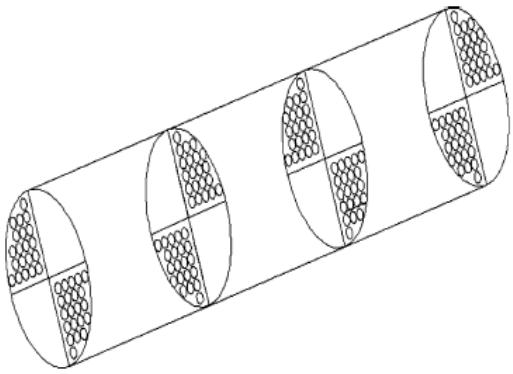

Fig. 2.2. Schematic of Flower baffle shell and tube heat exchanger.

Singh et al. (2013) performed an experimental analysis on the shell-and-tube heat exchanger containing segmental baffles at different orientations (Fig. 4). In the experimental study, three angular orientations (θ) of the baffles with 0º, 30º and 60º were considered for laminar flow with Reynolds number in the range 303 to 1516. It was observed that, with increase of Reynolds number from 303 to 1516, there was an increase in Nusselt number by 94.8% and 282.9% increase in pressure drop. Due to increase of Reynolds number from 303 to 1516, there is a decrease in non-dimensional temperature factor for cold water (ω) by 57.7% and hot water (ξ) by 57.1%, respectively.

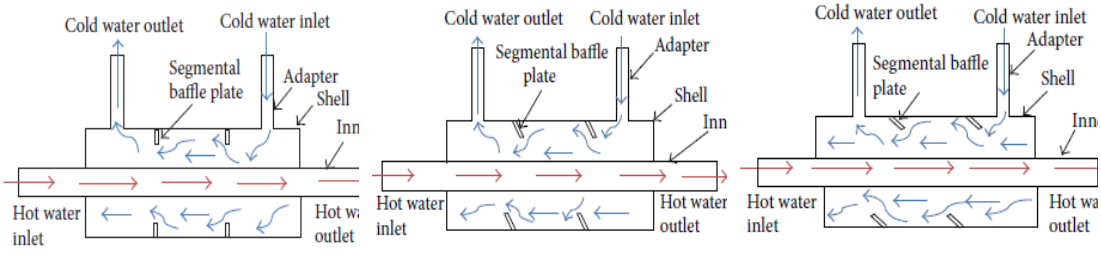

Fig. 2.3. Shell-and-tube heat exchanger having (a) 0°, (b) 30°, and (c) 60° baffle angles.

Khan et al. (2013) experimentally investigated shell and tube heat exchanger with helical baffles using aluminium oxide (II) nanoparticle. Al_2O_3 nano-particles are found to have good thermal conductivity for the heat transfer in shell and tube heat exchanger.

Al_2O_3 has been mixed with water as a base fluid to increase the heat transfer rate, using aluminium oxide (II) nanoparticle with two different volume concentrations 0.05% and 0.1%. The conclusion derived from the study is that overall heat transfer coefficient increases by increasing the concentration of nanoparticles in nanofluid up to certain level. The increase in heat transfer coefficient due to presence of Al_2O_3 nanoparticles is much higher than the conventional fluids and hence the shell and tube heat exchanger using nanofluid as a coolant has higher heat transfer rate than the conventional shell and tube heat exchanger.

Zhang et al. (2013) performed a pilot experimental study on shell and tube heat exchanger with small-angles helical baffles. In the study, the experimental comparisons of shell side thermodynamic and hydraulic performances were investigated among three helical baffles heat exchanger and one segmental baffles heat exchanger. The diameter of the heat exchanger was 500 mm and the effective tube length was 6 m. Focus of the study was to analyse the effect of helical angle (ranges from 7∘ to 25∘) on the performance of shell and tube heat exchanger. Among all the four heat exchangers, both the shell side heat transfer rate and the shell side pressure drop peak when helical angle equals 7◦, and the shell side heat transfer rate per unit pressure drop at this angle is the smallest. From the results, it can conclude that, for the same volume flow rate and same effective tube length with the increase of helical angle the shell side heat transfer coefficient for the helical baffles heat exchanger falls besides, the coefficient for the helical baffles scheme is bigger than that for the segmental scheme in the test angle range. The shell side heat transfer coefficient per unit pressure drop for the helical baffles is bigger than that for the segmental baffles, except the case with small helical angle (for example 7◦).

Anand et al. (2014) performed an experimental investigation of shell and tube heat exchanger using Bell Delaware method. The study was to analyse the heat transfer coefficient and pressure drops for different mass flow rates and inlet and outlet temperatures, using Bell Delaware method. This method takes in to account heat transfer by bypass and leakage streams, hence minimizing losses and providing more realistic estimates of heat transfer and pressure drops. Heat transfer coefficient and pressure drop were measured for both shell and tube sides with variation in mass flow rates. From the results, it is found that for the shell side with increase in mass flow rates

from 0.02 kg/s to 0.0397 kg/s, both heat transfer coefficient and pressure drop increases and for the tube side increase in mass flow rates from 0.015 kg/s to 0.0365 kg/s heat transfer coefficient decreases and pressure drop increases. It was also found that the overall heat transfer coefficient of the shell and tube heat exchanger increases with increasing flow rate.

2.2 Theoretical studies

Although, experimental studies are advantageous because of their realistic nature and represent actual phenomenon of the process involved in the physical problem, they have some limitations too. It becomes difficult and expensive to carry out experimental work in some cases for e.g. crash-landing analysis of aero-planes, heat transfer analysis of high temperature metal cooling process etc. Parametric variation is too difficult to carry out by experimental methods. These limitations can be overcome by using analytical or numerical analysis.

Costa et al. (2007), performed a study on design optimization of shell and tube heat exchanger. The formulated problem consists of the minimization of the thermal surface area for a certain service, involving discrete decision variables. Additional constraints represent geometrical features and velocity conditions which must be complied in order to reach a more realistic solution for the process task. The optimization algorithm is based on a search along the tube count table where the established constraints and the investigated design constraints are employed to eliminate non-optimal alternatives, thus reducing the number of rating runs executed. The performance of the algorithm and its individual components are explored through two design examples. The obtained results illustrate the capacity of the proposed approach to direct the optimization towards more effective designs, considering important limitations usually ignored in the literature.

Patel et al. (2010), studied the design optimization of a shell and tube heat exchanger using a non-traditional optimization technique called particle swarm optimization (PSO). This technique was used for design optimization of shell and tube heat exchanger from economical point of view. Three design variables such as shell internal diameter, tube outer diameter and baffle spacing along with two tube layouts (square and triangle) were considered for optimization. Four different case studies were

presented to demonstrate the accuracy and effectiveness of the proposed algorithm. In the PSO approach following upper and lower bounds for the optimization the following variables were imposed: shell inside diameter (D_s) ranging between 0.1-1.5 m; tubes outer diameter (d_o) ranging between 0.015-0.051 m; baffle spacing (B) ranging from 0.05-0.5 m. The results of optimization using PSO technique are compared with those obtained by using genetic algorithm (GA). Results shows a good agreement between PSO technique and genetic algorithm (GA).

Jozaei et al. (2012), performed a theoretical study to find the effect of baffles spacing on heat transfer, pressure drop and estimated price of shell and tube heat exchangers with single segmental baffles and tubes arranged in staggered layout. A program in EES (Engineering Equations Solver) software is used for this purpose to solve governing equations; moreover, Aspen B-JAC and HTFS$^+$ software were used for considering estimated total price. Simulated results obtained from this program were compared with experimental results for two different cases of baffle spacing. Baffle spacing from 4 to 24 inches were considered to find its effect on the ratio of overall heat transfer coefficient and pressure drop ratio ($U/\Delta p$). The results show that $U/\Delta p$ ratio is lower when baffle spacing is lower (i.e. 4 inches), this is due to the fact the pressure drop is higher for lower baffle spacing, even though overall heat transfer coefficient is significantly higher. In this case, it was found that the total price increased 7 %. Δp rapidly decreases and U decreases with the increase of baffle spacing, but the rate of decrease in U is lower than rate of decrease in pressure drop, so ($U/\Delta p$) ratio increases. After increasing baffles more than 12 inches, variation in pressure drop is gradual and approximately constant and U decreases; Consequently, $U/\Delta p$ ratio decreases again. If baffle spacing reaches to 24 inches, STHX will have minimum pressure drop, but U decreases, so required heat transfer surface increases and $U/\Delta p$ ratio decreases. After baffle spacing, more than 12 inches, variation of both estimated price and shell side pressure drop is negligible. So, optimum baffle spacing is suggested between 8 to 12 inches (43 to 63% of inside shell diameter) for a sufficient heat duty, low cost and low pressure drop.

Zhou et al. (2014), performed a theoretical study on prediction of temperature distribution in shell and tube heat exchanger and proposed an accurate and simplified model for predicting temperature distribution in the heat exchanger. The heat exchanger

is divided into a number of elements with tube side current in series and shell side current in parallel according to the baffle arrangement and tube passes. Two examples of BEU and AES heat exchangers with single-phase fluid are analysed to demonstrate the application and accuracy of the proposed model in temperature distribution prediction, compared with the Cell model and Heat Transfer Research Inc. (HTRI) method. The results show that the proposed model reproduces the temperature distribution given by the HTRI solution on the tube side flow with 0.19% accuracy for the BEU heat exchanger and 0.35% for the AES heat exchanger. It indicates that the prediction of the temperature distribution by the new model agrees reasonably well with that by HTRI method.

Jayachandriah et al. (2015), designed a STHX with helical baffles and compared its performance using Kern method with a STHX provided with segmental baffles. Then the geometric modelling is done by using CATIA V5 software. The model contains 7 tubes each having a diameter of 20 mm, length 500 mm and inner diameter of shell is 90 mm, length 600 mm. The material of the shell is considered to be Steel AISI 1010, Copper for tubes and Aluminium for baffles. The helix angle of baffle is varied from 0^o to 30^o. It was found from the results that the overall heat transfer coefficient is higher in STHX with helical baffles as compared to STHX with segmental baffles. The pressure drops decreases with the increase in helix angle. STHX with helical baffles with helix angle of 6^o provide better heat transfer than the baffles with helix angle of 18^o. Lower is the helix angle lower will be the pumping cost.

Bhuyian et al. (2016), performed a theoretical review study on thermal and hydraulic performance of finned tube heat exchangers under different flow ranges. In this study, different experimental/numerical investigations were reviewed, grouped and summarized based on the types of heat exchangers, heat transfer and pressure drop performance, effects of geometrical parameters under different flow conditions. Overall, this study highlights the existing technologies and emerging trends in designing finned-tube heat exchangers considering different arrangements and geometric parameters under variable flow conditions which will be helpful for selecting appropriate design depending on the requirement.

2.3 CFD Studies

In recent years, numerical analysis using CFD become popular to address different fluid flow and heat transfer problems owing to its accuracy and easiness in parametric variations. In this method, fluid flow and heat transfer can be visualized and calculated using distributions of velocity, temperature, pressure etc. Further it became easier to present the results in a better way by using animated profiles.

Ozden et al. (2010), performed a shell side CFD analysis of a small shell and tube heat exchanger. The shell side design of a shell-and-tube heat exchanger; in particular, the baffle spacing, baffle cut and shell diameter dependencies of the heat transfer coefficient and the pressure drop are investigated. The flow and temperature fields inside the shell are resolved using a commercial CFD package. A set of CFD simulations is performed for a single shell and single tube pass heat exchanger with a variable number of baffles and considering the flow as turbulent. The results were found to be sensitive to the turbulence model used. The best turbulence model among the ones is determined by comparing the CFD results of heat transfer coefficient, outlet temperature and pressure drop with the Bell–Delaware method results. The effect of the baffle spacing to shell diameter ratio on the heat exchanger performance is investigated for two baffle cut values at different flow rates. Three turbulence models using two different mesh densities were tried for the first and the second order discretization. By comparing with Bell–Delaware results, the *k*-ε realizable turbulence model with the first order discretization and the fine mesh is selected as the best simulation approach. The simulation results were compared with the results from the Kern and Bell–Delaware methods by considering the baffle spacing between 6 to 12, baffle cut values 36% and 25%, shell side flow rates as 0.5, 1 and 2 kg/s. It was observed that the Kern method always under predicts the heat transfer coefficient. It is observed that the CFD simulation results were in very good agreement with the Bell–Delaware results for properly spaced baffles. The results were also found to be sensitive to the baffle cut and heat exchanger with 25% baffle cut gives slightly better results. The differences between Bell–Delaware and CFD predictions of the total heat transfer rate were below 2% for all the cases.

Alawa et al. (2012), performed numerical analysis to find the heat transfer characteristics in heat exchangers. In this study, a numerical method of solution, capable

of accounting variations of fluid properties with temperature and heat transfer was presented. Field data were collected for three different industrial heat exchangers (1, 2 and 3) and the heat transfer analysis was carried out by applying basic conservation principles. The parameters analysed include: the outlet temperatures, the heat transfer coefficients and the heat exchanger effectiveness. The tube side outlet temperature deviation between numerical results and field data for the heat exchangers 1, 2 and 3, were found to be 0.53%, 0.11% and 5.10% respectively. The shell side outlet temperature deviation was 0.76%, 0.47% and 0.74%. Comparison of the calculated and actual overall heat transfer coefficients gave deviations of 8.7%, 7.77% and 11% for exchangers 1, 2 and 3 respectively.

Chalwa et al. (2013), studied the variation of pressure drop and temperature distribution in a shell and tube heat exchanger with vertical baffles. Numerical analysis was carried out using CFD and validated with experimental results considering baffle spacing, baffle cut as the design parameters. It concluded from the results that the flow characteristics become independent of the baffle cut. Heat transfer rate on the shell side varied with baffle cut which in turn affected the tube side heat transfer rate. Rate of heat transfer decreased from 3 to 25% and pressure drop increased 3 to 25%, with the increase in the baffle cut. Velocity gradually increased from entry to exit point of the heat exchanger on shell side.

Saffarian et al. (2014), performed a numerical analysis of shell and tube heat exchanger with simple baffles using CFD. In the study, the heat exchanger with a shell length of 5.85 m and shell diameter of 200 mm is considered. The heat exchanger consists of 37 tubes and 4 baffles inside the shell. Flow and temperature fields were analysed inside the shell and the tubes using CFD software. k-ω SST model was used for investigation as it gives better results for turbulence modelling. The analysis was carried with three different meshes: coarse, medium and fine and after grid independence test a mesh consisting 4.2 million elements was used. Numerical results were presented in the form of profiles of temperature and velocity and were compared with experimental data. It was found that flow becomes more turbulent with the use of baffles and as a result the heat transfer coefficients were increased.

Yang et al. (2014) conducted the comparison of four different numerical modelling approaches for enhanced rod baffled shell and tube heat exchanger and validated the results with experimental data. The four methods of numerical modelling include the unit model, the periodic model the porous model and the whole model. In first two a small subsection of heat exchanger was modelled, third one in which heat exchanger was considered as porous medium and in the last model the entire heat exchanger was modelled with CFD. It was concluded from the results that the periodic model, porous model and the whole model can have high accuracy in predicting heat transfer, while the unit model has relatively less accurate. The porous and the whole model also provide good idea of pressure drop but the unit model and periodic model fail to predict pressure drop accurately. The experiments validate the precision of each model in predicting heat transfer and pressure drop with the experimental validation.

You et al. (2015), carried out a study of numerical simulation and performance improvement for a small size shell and tube heat exchanger with trefoil-hole baffles and validated with experimental data. Structural modification was made on heat exchanger and the effect of baffles distance on thermo-hydraulic performance was investigated. Numerical results demonstrate that with the structural modification, the pressure loss on the shell side decreases by 21% and the shell side overall thermos-hydraulic performance increases by 21.9%. In addition, the convection heat transfer coefficient on the shell side was observed to be decreasing monotonically with the decrease in number of baffles, while the variation tendency of overall thermo-hydraulic performance with number of baffles number is opposite.

Wang et al. (2015), carried out an experimental and numerical investigation on performance comparison for shell and tube heat exchangers with different baffles. An improved structure of ladder type fold baffles was proposed to block the triangular leakage zones in original heat exchangers with helical baffles. The numerical results show that the distribution of velocity and temperature on shell side in improved heat exchanger were more uniform and axial short circuit flow was eliminated. The experimental results show that the shell side heat transfer coefficient and overall heat transfer coefficient were improved by 22.3-32.6% and 18.1-22.5% respectively. The increase in shell side pressure drop was about 0.911-9.084 kPa, while the corresponding pumping power penalty was about 2-80 W. The thermal performance factor enhanced

by 18.6-23.2%, which clearly indicate that the ladder type fold baffles can effectively improve the heat transfer performance of heat exchanger compared with helical baffles.

Joemer et al. (2015), performed a numerical simulation for optimization of shell and tube heat exchanger for maximum heat transfer by the optimizing the baffle inclination and baffle cut. The performance of the shell and tube heat exchanger were studied by varying the parameters using CFD software package ANSYS FLUENT. Experiment analysis was conducted to validate the CFD results on an existing single pass counter flow shell and tube heat exchanger. The initial baffle angle was 0° and later this was varied to, 10°, 15° and 20°. The initial baffle cut was 20% and later this was varied to 20%, 25% and 30%. It was observed that the heat transfer was changing with the baffle angle and baffle cut. The maximum heat transfer was found to be 5047.68W obtained for 5° of baffle angle and 25% of baffle cut. Optimized model has maximum turbulent intensity compared to other arrangements.

Eshita et al. (2016), performed CFD simulations of a shell and tube heat exchanger with and without baffles for different mass flow rates. In this study, an attempt has been made to investigate the complex flow and temperature pattern in a small shell and tube heat exchanger with and without baffles. It was concluded that the conventional heat transfer correlations are not applicable for the analysis of small heat exchangers as flow near the nozzle significantly contributes to the heat transfer hence the conventional heat transfer correlations do not apply to these small sized heat exchangers. It was also observed that k-$\mathcal{E}$ model with standard wall function gives best results for velocity profile as well as heat transfer compared to the other models. A sensitivity study of exit length was also conducted and it was found that exit length to shell side velocity ratio must be 2.5 for proper convergence.

Ambekar et al. (2016), performed numerical study using CFD for a shell and tube heat exchanger including baffles with different segment configurations. Different baffles configurations include single, double and triple segmental baffles, helical baffles and flower baffles were considered. It was found that single segmental baffle gives better overall heat transfer coefficients but with large pressure drop thus consumes large pump power. Numerical results show that for constant shell side mass flow rate, heat transfer coefficient, heat transfer rate and pressure drop is higher for single segmental baffles.

Pressure drop observed to be 70-75% with double segmental baffles and 65-70% with helical baffles was higher than that with single segmental baffles. Flower baffles reduces the pressure drop by 25-35% than single segmental baffles.

Shahril et al. (2016), carried out a thermo-hydraulic performance analysis of a shell and double concentric tube heat exchanger (SDCTHEX) using CFD. Performance of the SDCTHEX (Fig. 5) having fixed inner tube diameter is compared with classical shell-and-tube heat exchanger (STHEX) for different mass flow rates of the hot fluid. Further the effects of different inner tube diameters on the performance of SDCTHEX were also investigated. The numerical results show that the average percentage increase in overall heat transfer rate per overall pressure drop of SDCTHEX with inner tube diameter equal to 8/12 mm/mm, is nearly 343% higher than that of STHEX while the total friction power expenditure of SDCTHEX is reduced by around 85.5% as compared to that of STHEX. Also, the overall heat transfer rate per overall pressure drop of SDCTHEX is sensitive to inner tube diameter. It is found that $U/\Delta p$ for the mass flow rate of 22.5 kg/s is more and found to be about 400% higher at inner tube diameter of 12/16 mm/mm with respect to the STHEX. The results of simulation present that, the SDCTHEX has a higher heat transfer performance while maintaining a lower pressure drop. It was also found that higher effectiveness may be achieved at lower inner tube diameters as well with higher hot fluid mass flow rates which would be economical. This suggests that the SDCTHEX might be ideal choice to replace the classical STHEX in heat exchanger industrial applications.

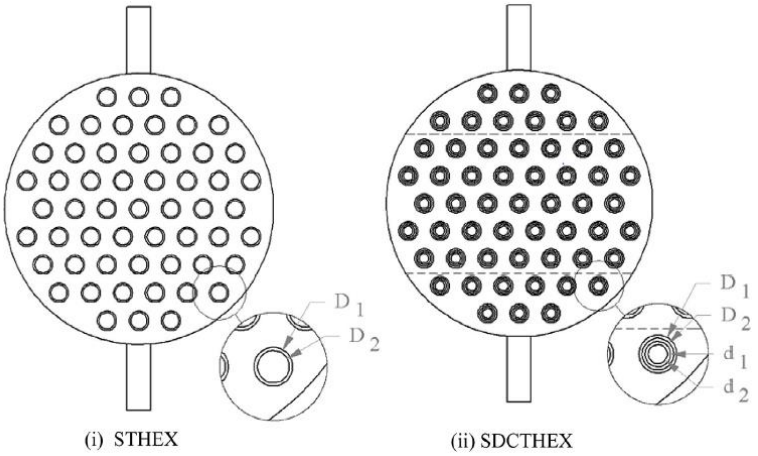

Fig. 2.4. Tubes arrangement inside Shell-and-tube heat exchanger.

2.3 Observations and recommendations based on literature review

Following are the observations on the basis of literature survey performed on solar thermal energy conversion system

- Most of the studies were related with the design parameters of solar FPC and SHTX.
- Number of baffles, baffle cut and baffles spacing had been used by the researchers to find out their effect on heat transfer coefficients and pressure drop and for solar FPC optimum tilt angle, collector design, fluid flow rate, thermal insulation, finned tube, twisted round tubes etc. parameters has been evaluated to optimize its performance.
- Many researchers have validated their experimental results with CFD simulations and concluded that CFD results are close to the experimental results. Thus, the CFD model can be used for further study of solar thermal energy conversion system for both design and performance optimization.
- It was found that shell side both heat transfer coefficient and pressure drop increases with the increase in shell side mass flow rate. Whereas, with the increase in mass flow rate on tube side the tube side heat transfer coefficient decreases and the tube side pressure drop increases. It was also found that the overall heat transfer coefficient of the shell and tube heat exchanger increases with increasing shell side mass flow rate.
- It was found that increase in mass flow rate decrease the outlet temperature of fluid and increase in solar radiation increases the outlet temperature of the fluid and vice-versa. So, to achieve optimum efficiency moderate values of mass flow rate and solar radiation must be maintained.
- Use of different types of baffles like helical baffles with inclination angles, flower baffles and vertical baffles can play a major role in performance enhancement of shell and tube heat exchanger.
- Leakage losses of shell and tube heat exchangers can be minimised by introduction of sealers and thus overall performance can be improved.

Chapter 3

CFD simulation modelling

In last thirty years of development of the Computational Fluid Dynamics (CFD) tool has made it possible to get a better understanding, analysis and solution of the fluid flow and the heat transfer problem in many applications. Analysis and simulation of heat exchanger units can be performed quite accurately with the help of CFD. Further, increasing computational power has enabled the researchers to create three-dimensional model using a fine grid for obtaining more accurate results.

CFD computer programs can be used to predict the fluid flow behaviour. The majority of the CFD programs are based on the solution of the Navier-stokes equations, the energy equation. CFD tools gives a detailed knowledge of the pattern of heat transfer and the distribution of flow and temperature within a heat exchanger, so the applications of CFD tools have become important due to deep-informative results with relatively less efforts and equipment costs involvement. CFD analysis is generally performed by using the commercial software FLUENT, PHOENIX, CFX etc. to name few of them, which work on finite volume method (FVM) based code for fluid flow simulations.

3.1 Overview of CFD simulation modelling

CFD codes are structured around the numerical algorithms that can tackle fluid flow problems. In order to provide easy access to their solving power all commercial CFD packages include sophisticated user interfaces to input problem parameters and to examine the results. Hence the codes contain three main elements: (i) a pre-processor, (ii) a solver and (iii) a post-processor. The function of each of these elements within the context of a CFD code is explained in the following paragraphs.

3.1.1 Pre-processor

Pre-processing consists of the input of a flow problem to a CFD programme by means of an operator-friendly interface and the subsequent transformation of this input onto a form suitable for use by the solver. The user activities at the pre-processing stage involve:

- Definition of the geometry of the region of interest: the computational domain.

- Grid generation – the sub division of the domain into a number of smaller, non-overlapping, sub-domains; a grid or mesh of cells that act as control volume or elements.
- Selection of the physical and chemical phenomenon that need to be modelled.
- Definition of thermos-physical properties of fluids involved.
- Providing specifications of appropriate boundary conditions at cells which coincide with or touch the boundaries of domain being analysed.

The accuracy of a CFD simulation if governed by the number, shape and size of the cells in the grid. In general, larger the number of cells, better is the solution accuracy. Both, the accuracy of a solution and its cost in terms of necessary computer hardware and calculation time, are dependent on the fitness of the grid. Optimal meshes are often non-uniform: finer in areas where large variations occur from point to point and coarser in regions with relatively little change. A CAD system is required for geometric modelling and grid generation.

3.1.2 Solver

In this stage, numerical algorithms are used for solving the different equation of fluid flow and heat transfer. Finite volume method is most commonly used in CFD analysis. The numerical algorithm consists of the following steps:

- Formal integration of the governing equations of fluid flow over all the (finite) control volumes of the solution domain.
- Discretization involves the substitution of a variety of finite-difference type approximations for the terms in the integrated equation representing flow processes such as convection, diffusion and sources. This converts the integral equation into a system of algebraic equations.
- Solution of the algebraic equation by iterative method.

3.1.3 Post-processor

Over past few years, a huge amount of development work has taken place in the field of post-processing CFD analysis. Owing to the increased popularity of engineering workstations, many of which have outstanding graphics capabilities, the leading CFD packages are now equipped with the versatile data visualization tools. These include:

- Domain geometry and grid display
- Vector plots
- Line and shaded contour plots
- 2D and 3D surface plots
- Particle tracking
- View manipulation (translation, rotation, scaling etc.)
- Colour postscript output
- Animation for dynamic result display

All commercially available codes produce trusty alphanumeric output and have data export facilities for further manipulation external to the codes.

3.2 Problem solving steps in CFD

Having determined the important feature of the problem to be solved, then the following basic procedural steps should be followed:

i. Create the model geometry in the SOLIDWORK
ii. Start the FLUENT by selecting the appropriate solver for 3D modelling
iii. Import the geometry from SOLIDWORKS to FLUENT
iv. Create grid in meshing
v. Select the solver formulation
vi. Choose the basic equations to be solved: laminar or turbulent, energy equation, heat transfer models etc.
vii. Specify material properties.
viii. Specify the boundary conditions
ix. Adjust the solution control parameters, initialize the flow field and calculate a solution by iteration
x. Examine and write the results
xi. Validate CFD results with experimental or any other results such as mathematical modelling results or results published by any other researchers
xii. If necessary, refine the grid or consider revision to the numerical or physical model.

The geometric model created in SOLIDWORKS is imported in FLUENT and grid is created in meshing. A numerical solver (e.g. density based, pressure based, unsteady

etc.) is selected based upon the type of fluid flow and heat transfer mechanism. Appropriate physical models (turbulence, combustion, multiphase etc.) are selected depending upon type of application.

Properties of the material to be used in CFD analysis are defined and then operating and boundary conditions are specified at all boundary zones. Solution control parameters like pressure velocity coupling, discretization scheme, convergence criteria etc. are defined.

After initializing the flow field, calculation for the solution is started using iteration interface provided in FLUENT. The solution which is obtained by CFD simulation should be validated with the experimental results of mathematical modelling or previously published results of similar problem before using the results of CFD simulation.

3.3 CFD model development and simulation

CFD model development includes modelling and meshing of shell and tube heat exchanger, assumptions, turbulence model, energy equations, numerical solver, solution techniques, and pressure velocity coupling etc.

3.3.1 Geometrical model and meshing of shell and tube heat exchanger

The geometric model of shell and tube heat exchanger was prepared using SOLIDWORKS version 15. This model prepared using dimensions based on analytical calculations performed for designing purpose of shell and tube heat exchanger. Then meshing of generated model is carried out using ANSYS MESH.

Two shell and tube heat exchangers one with aligned grid and other one with staggered grid was modelled having 21 and 24 number of tubes respectively. Dimensions for both the heat exchangers were similar. The geometry of the shell and tube heat exchanger as shown in figure 4.1 consists shell of diameter 9.47 cm, tube outer diameter 12.5 mm, tube inner diameter 11 mm and tube length 81.01cm. A circular inlet and outlet of 15 mm diameter is provided on both shell and tube inlets and outlets. 24 copper tubes of length same as shell length are arranged in staggered manner inside the shell. Staggered arranged tube having horizontal and vertical pitch of 1.5625 cm and diagonal pitch as 0.78125 cm whereas aligned grid has pitch of 1.5625 cm for both horizontal as well as

diagonal. Number of baffles used in heat exchanger is 2 having baffle distance of 29.2 cm and 51.5 cm respectively from the end of tube fluid inlet.

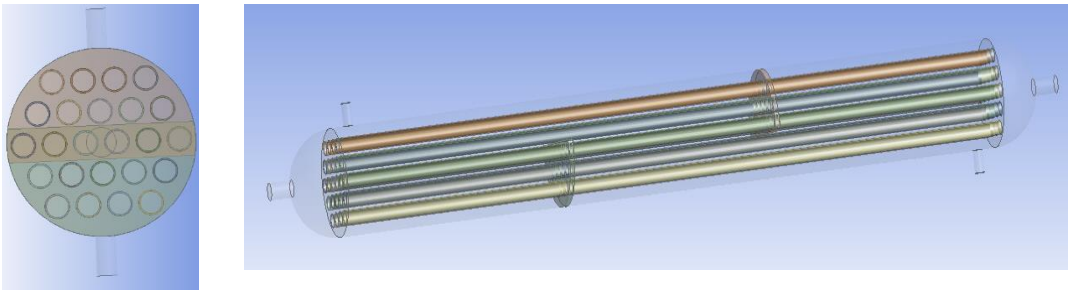

Fig. 3.1: Geometry of Shell and tube heat exchanger with staggered grid.

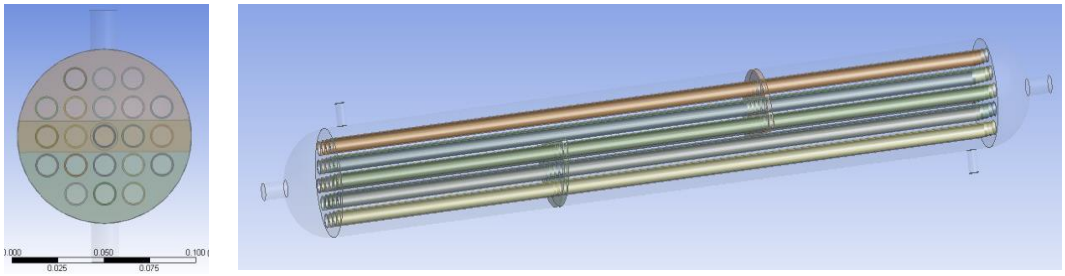

Fig. 3.2: Geometry of Shell and tube heat exchanger with aligned grid.

Figure 3.3 shows the cell distribution for shell and tube heat exchanger. A structured mesh distribution has grid lines on 3-coordinate directions, in which they are unlikely to be orthogonal in physical space but they can be treated as orthogonal in computational space. Each cell of structured mesh distribution is topologically like a hexahedron. These structured mesh distributions make mesh generations practically very difficult for real life application for other than simple geometry. But an unstructured mesh distribution is not restricted in this way and shape of the cell can be hexahedral, tetrahedral or wedge shaped and in computational domain unstructured mesh distribution is not orthogonal. Hence, finally it was decided to use unstructured mesh distribution for shell and tube heat exchanger. Although, structured meshes are less computationally intensive than unstructured meshes, but they become quite complicated for the applications other than simple cases and the use of structured meshes is restricted in simple geometries.

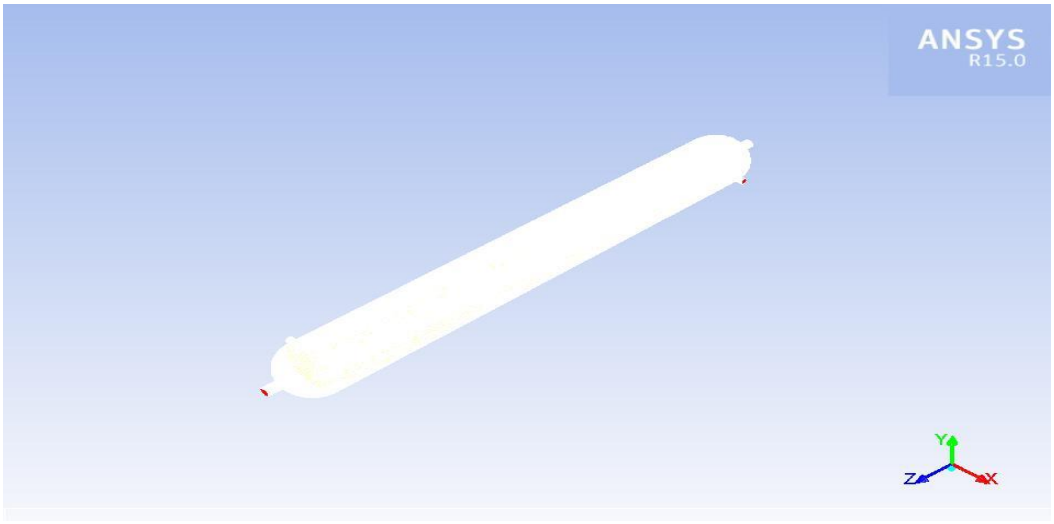

Fig. 3.3: CFD model of shell and tube heat exchanger

The geometry shown in figure 4.2 has been generated for the analysis of shell and tube heat exchanger. Figure 4.3 shows the meshed geometry in which face and shell is shown. For mesh, at 0.017 interval size number of elements was 17622730 created.

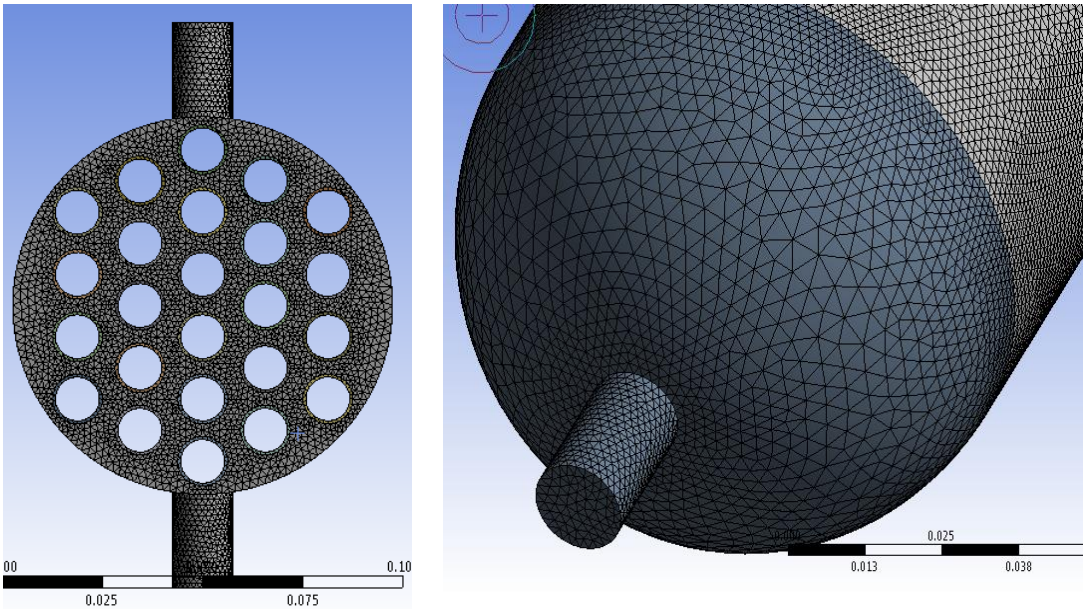

Fig. 3.4: Mesh generated in shell and tube heat exchanger with staggered tube

3.3.2 Geometrical model and meshing of solar flat plate collector

The geometric model of solar flat plate collector was prepared using SOLIDWORKS version 15.0. This model was prepared using dimensions of existing model of solar flat plate collector used earlier in MNIT Jaipur.

Geometry of solar flat plate collector as shown in fig. 3.5 has length of 2 meters, width of 1 meters and thickness of absorber plate is 4 mm. Total 9 Absorber tubes having inner diameter of 11 mm and outer diameter of 12.5 mm were modelled.

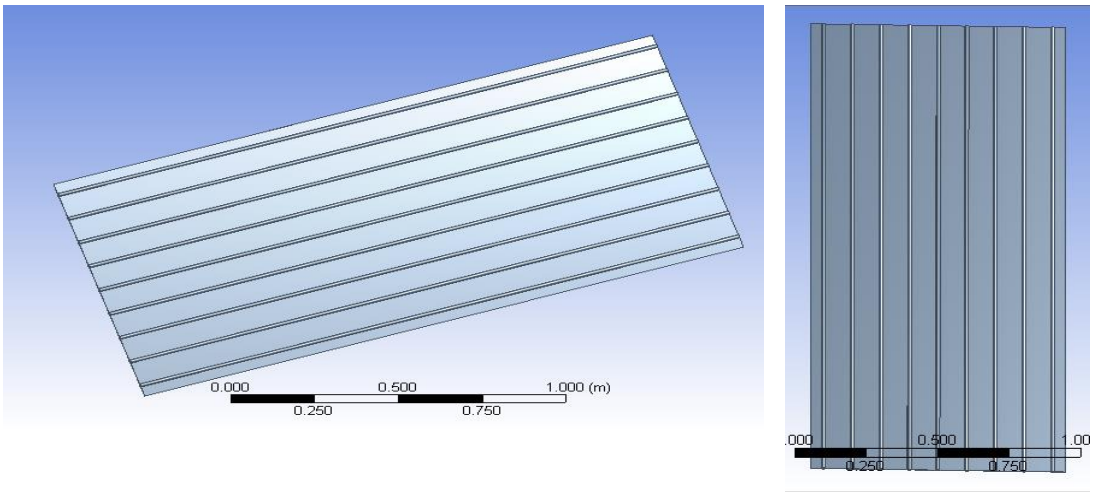

Fig. 3.5: Geometry of solar flat plate collector

Figure 3.6 shows the meshed geometry of solar flat plate collector in which tube inlet face and absorber plate surface is shown. For mesh, at 0.012 interval size number of elements was 897902 created.

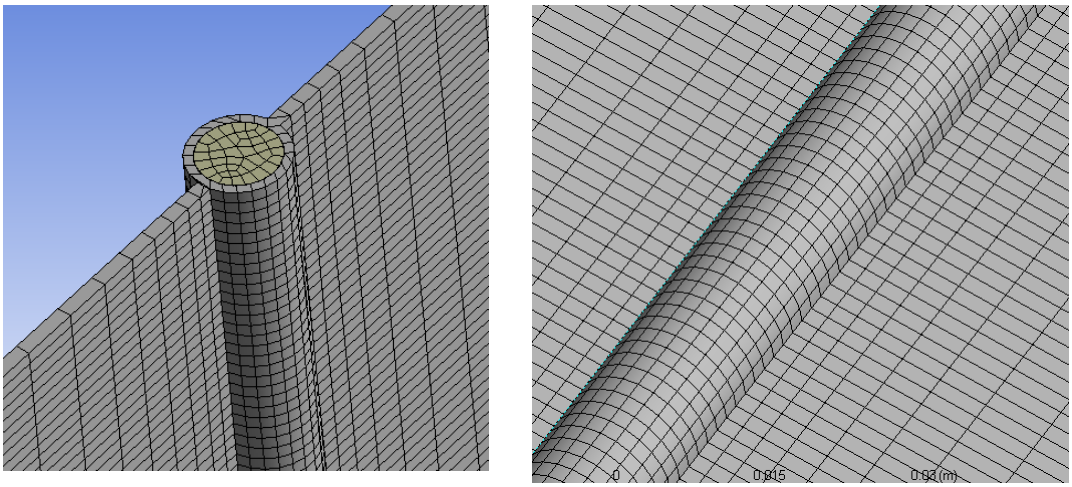

Fig. 3.6: Mesh generated in solar flat plate collector

In the CFD analysis, FLUENT version 15.0 [ANSYS. Inc] has been used and the FLUENT computation adopts a finite-volume approach to solve the conservation form of the governing flow equations on the unstructured meshes. The fundamental equation of the fluid such as Navier-stokes equations, continuity equations and heat transfer, used in FLUENT are described in Appendix A-1.

3.3.3 Assumptions

Assumptions considered in CFD simulation modelling are as follows:

i. Velocity and temperature at the entrance of the inlet at shell and tube heat exchanger and solar flat plate collector for water is uniform.
ii. No flow leakages occur in the system. Side walls of the system are considered adiabatic walls are considered at side of the system.
iii. The thermal conductivity of the solid material is constant.
iv. No internal source exists for thermal-energy generation in shell and tube heat exchanger.
v. There is no phase-change throughout the heat exchanger.
vi. Properties of the fluids and the wall, such as specific heat, thermal conductivity, and density are only dependent on temperature.
vii. Simulation is done at no wind condition means only free convection is considered.

3.3.4 Numerical solver used

FLUENT has major numerical solvers; namely, segregated solver and coupled solver (implicit and explicit type). FLUENT solve the governing integral equations for the conservation of mass, momentum and energy (when appropriate). Apart from these equations other equations involving scalar quantities such as turbulence and chemical species can also be solved in FLUENT and in all the cases a control volume based technique is used. In the present study, segregated solver was used. In the segregated algorithm, the individual governing equation for the solution variables (velocity, temperature, pressure, turbulent kinetic energy, etc.) are solved one after another. Each governing equation, while being solved, is “decoupled” or “segregated” from other equation. The segregated algorithm is memory-efficient, since the discretized equations

need only be stored in the memory one at a time. Due to memory efficiency of the solver, it has been considered in the present case.

In this CFD analysis, only water is flowing from both shell and tube inlet to outlet. There is heat transfer between tube fluid and shell fluid. By defining appropriate operating conditions, boundary conditions, solution parameters and convergence criteria, a converged numerical solution is obtained for each step. Different solution and geometric variable such as tube alignment, tube fluid mass flow rate and shell fluid mass flow rate were analysed in each step using the sequential result of the CFD simulation.

3.3.5 Solution technique

Solution of the equations governing scalers (e.g. Temperature, pressure, velocity) requires a discretization scheme. According to Fluent user guide (Fluent Incorporated) the First Order Scheme gives a suitable solution with a good rate of residual convergence, with the limitation that the accuracy of the solution may not be satisfactory while the Second Order Upwind scheme will result into more accurate solution. In this simulation First Order Upwind on all variables has been used to achieve residual convergence. The k-ε model was applied with the first order upwind discretization scheme in combination with the standard wall function.

3.3.6 Turbulence model

The largest challenge of CFD modelling was correct analysis of turbulent flow. It is characterized in terms of irregularity, diffusivity, large Reynolds number, three-dimensional vorticity fluctuations, dissipation and continuum.

Because water flows through the shell and tubes of heat exchanger which have larger Reynolds number can be defined as turbulent ones, the CFD programs used for water flow analysis and prediction requires appropriate models for turbulence.

The two-equation model, often referred to as the k-ε model, is the most-widely used turbulence model in engineering practice. Here, k represents the turbulence kinetic energy, while ε represent the dissipation rate of turbulence energy. There are many factors that influence the results such as mesh generation, convergence procedure and

boundary condition implementation. Therefore, a more powerful computer and a skilful user are necessary for an effective and accurate simulation.

Based upon the above fact the k-ε model is most suitable this study. In this CFD analysis RNG k-ε model has been used for analysing the water flow inside shell and tube heat exchanger because this model support swirl dominated flow and viscous heating. A brief description of the turbulence transport equation for the RNG k-ε is given in Appendix A-1.

3.3.7 Pressure velocity coupling

The SIMPLE pressure-velocity-coupling scheme was used in this CFD analysis for problem in this case.

3.3.8 Input Parameters

Thermos-physical properties including density, thermal conductivity and specific heat capacity of the materials, used for CFD simulation of shell and tube heat exchanger shown in table 4.1. Flow operating parameters used in the present CFD simulation are mass flow rate and temperature of water at inlet of shell and tubes.

i. Materials

Water property was selected from a database stored within fluent. Properties of copper were also selected form the same database of fluent.

Table 3.1: Thermo-physical properties of material

S. No.	Material	Density (kg/m^3)	Specific heat capacity (J/kg-K)	Thermal conductivity (W/m-K)
1	Water	998.2	4182	0.6
2	Copper	8978	381	387.6

ii. Boundary Conditions

In this section, the type of boundary condition for each of the physical boundaries of the shell and tube heat exchanger is explained.

(a) Inlet conditions

Velocity inlet has been specified at the shell fluid inlet and cold fluid inlet since the velocity of the inlet was known. Default values are taken for turbulent kinetic energy (k) and kinetic energy dissipation rate. Temperature values are also specified.

(b) Outlet conditions

The outlet type "outflow" was specified for this simulation. It is the appropriate outlet boundary condition for cases where the flow is fully developed, i.e. where there is no significant variation of the flow variables in the flow direction. Flow rate weighting values are also specified.

(c) Walls

Zero heat flux conditions have been used for all walls other than the shell fluid and tube fluid walls of shell and tube heat exchanger. Shell fluid and tube fluid walls thickness is considered very low and convection heat transfer is considered from these walls. Baffles walls were taken as solid and considered as no heat flux. Default values like wall roughness and wall motion are taken.

3.3.9 Convergence

To reach convergence, residuals were monitored for X, Y and Z velocity, continuity, energy, turbulent kinetic energy (k) and kinetic energy dissipation rate. The convergence criterion for all the variables is 10^{-3} except for energy, the convergence criteria for energy is 10^{-6}.

3.3.10 Results of CFD Simulation

a) Numerical simulation was carried out to analyse the effect of tube arrangement in the shell and tube heat exchanger. Two heat exchangers of same dimensions were modelled having 24 and 21 number of tubes arranged in staggered in aligned manner respectively.

   Based on the results shown above, LMTD and Effectiveness was calculated for aligned and staggered tube heat exchanger. LMTD for staggered and aligned tube heat exchanger is 32.85°C and 39.28°C respectively. Effectiveness for staggered and aligned tube heat exchanger is 64.10% and 53.15%. Based on effectiveness it is clear that staggered tube heat exchanger is more efficient than aligned tube heat exchanger, so further calculations were performed on staggered tube heat exchanger.

Table 3.2: Temperature results of shell and tube heat exchanger

S. No.	-	SHTX with Aligned grid	SHTX with Staggered grid
1	Shell fluid inlet	20°C	20°C
2	Shell fluid outlet	35.33°C	42.93°C
3	Tube fluid inlet	85°C	85°C
4	Tube fluid outlet	50.45°C	43.33°C

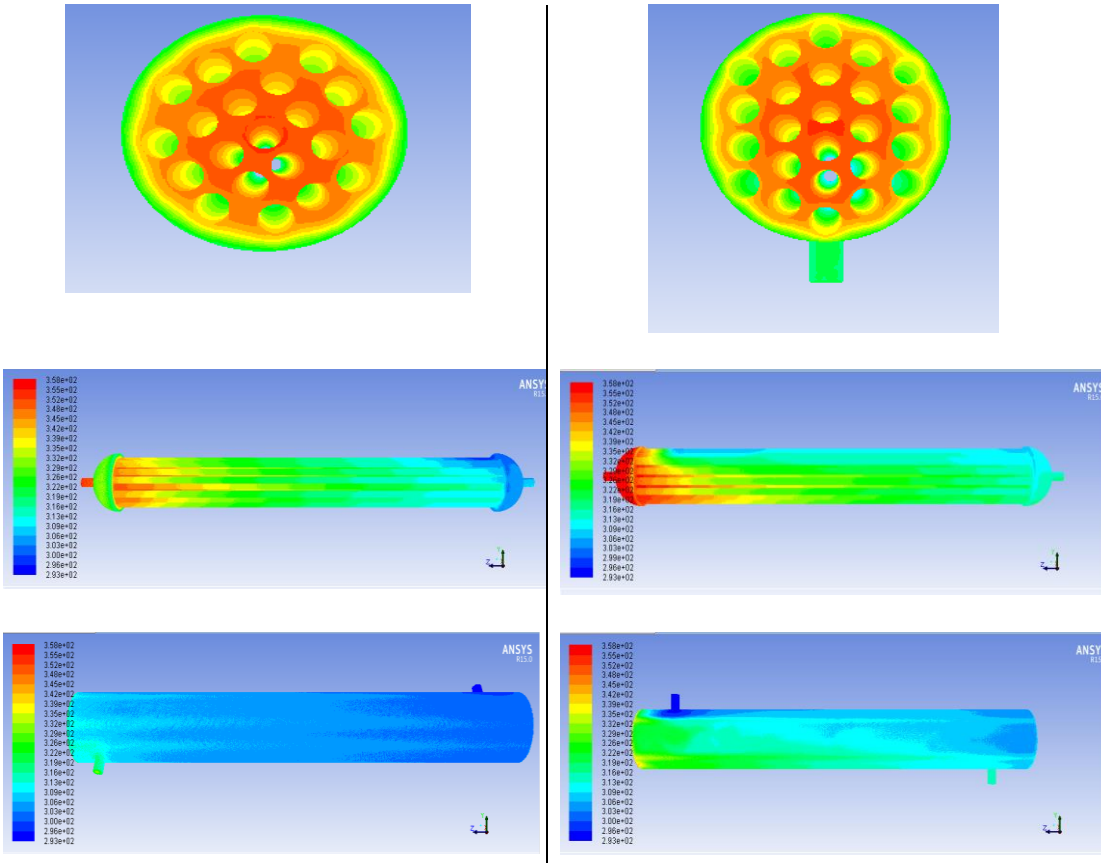

(a) Shell and tube heat exchanger with aligned grid **(b) Shell and tube heat exchanger with staggered grid**

Fig. 3.7 Static temperature variation in shell and tube heat exchanger (a) with aligned grid, (b) with staggered grid

b) Results for solar flat plate collector has been presented in table 3.3.

Table 3.3: Temperature results of solar flat plate collector

Solar radiation (W/ m^2)	Inlet velocity (m/s)	Inlet water temp. (°C)	Outlet water temp. (°C)	Surface temp. (°C)
850	0.025	20°C	38.17°C	81.42°C

3.4 Validation of CFD results for shell and tube heat exchanger

The CFD model developed has been validated against the experimental investigations carried out on an experimental setup of shell and tube heat exchanger with staggered tube arrangement at MNIT Jaipur (Rajasthan). Numerical simulation was carried out with keeping the shell and tube side mass flow rate as 200 kg/hr and 150 kg/hr respectively. Results of comparison of shell and tube fluid outlet are presented:

Table 3.4: Comparison of experimental and CFD results for STHX.

-	Experimental	CFD
Shell fluid inlet	34.9°C	35°C
Shell fluid outlet	38.4°C	40.1°C
Tube fluid inlet	79.1°C	80°C
Tube fluid outlet	40°C	41.6°C

It is observed from the comparison of the results that the variation in simulated results with respect to the experimental outlet fluid temperatures ranges between 0.28% to 4.43% which shows good agreement between simulated results and experimental observations.

Since the comparison shows the good agreement between simulated results and experimental observations, the model is a valid model and can be used for parametric analysis, optimization and performance study of shell and tube heat exchanger and solar flat plate collector.

Chapter 4

Parametric analysis and performance study

The CFD model was developed for solar flat plate collector and shell and tube heat exchanger and validated with experimental results. This validated model has been used to study the effect of various parameters of solar flat plate collector and shell and tube heat exchanger on its performance. With the help of parametric analysis solar thermal energy conversion system has been optimized.

It is found from the previous research that various parameters of the solar flat plate collector such as mass flow rate and solar radiation affects the thermal performance of solar collector. So, in this study these important parameters are considered for CFD simulation. For the existing solar flat plate collector, variation of mass flow rate has been considered for studying thermal performance of Solar FPC system.

4.1Effect of mass flow rate on performance of Solar FPC

Different mass flow rates ranging from 0.001 kg/s to 0.01 kg/s have been considered for CFD simulation to study its effect on fluid outlet temperature and useful heat gain. Other parameters such as solar radiation and inlet air temperature are taken constant. Water outlet temperature, heat gain and efficiency at different mass flow rates are calculated from CFD simulation and these are shown in table 4.1 to 4.5.

Table 4.1: simulated results for outlet temperature and heat gain at m_f = 0.001 kg/s

S. No.	Solar Radiation (W/m^2)	Temperature (°C)			Heat gain (W)
		Inlet water	Outlet water	Temp. rise	
1	500	20	46.68	26.68	111.469
2	600	20	52.02	32.02	133.779
3	700	20	57.33	37.33	155.964
4	800	20	62.695	42.695	178.3797
5	900	20	68.03	48.03	200.669
Average			**57.35**	**37.35**	**156.052**

Table 4.2: simulated results for outlet temperature and heat gain at m_f = 0.0025 kg/s

S. No.	Solar Radiation (W/m^2)	Temperature (°C)			Heat gain (W)
		Inlet water	Outlet water	Temp. rise	
1	500	20	30.68	10.68	111.55
2	600	20	32.82	12.82	133.91
3	700	20	34.95	14.95	156.15
4	800	20	37.10	17.10	178.61
5	900	20	39.24	19.24	200.96
Average			**34.958**	**14.958**	**156.236**

Table 4.3: simulated results for outlet temperature and heat gain at m_f = 0.005 kg/s

S. No.	Solar Radiation (W/m^2)	Temperature (°C)			Heat gain (W)
		Inlet water	Outlet water	Temp. rise	
1	500	20	25.35	5.35	111.76
2	600	20	26.41	6.41	133.90
3	700	20	27.48	7.48	156.25
4	800	20	28.56	8.56	178.82
5	900	20	29.63	9.63	201.17
Average			**27.486**	**7.486**	**156.38**

Table 4.4: simulated results for outlet temperature and heat gain at m_f = 0.0075 kg/s

S. No.	Solar Radiation (W/m^2)	Temperature (°C)			Heat gain (W)
		Inlet water	Outlet water	Temp. rise	
1	500	20	23.56	3.56	111.55
2	600	20	24.27	4.27	133.80
3	700	20	24.99	4.99	156.36
4	800	20	25.70	5.70	178.60
5	900	20	26.42	6.42	201.17
Average			**24.988**	**4.988**	**156.29**

Table 4.5: simulated results for outlet temperature and heat gain at m_f = 0.01 kg/s

S. No.	Solar Radiation (W/m^2)	Temperature (°C)			Heat gain (W)
		Inlet water	Outlet water	Temp. rise	
1	500	20	22.67	2.67	111.55
2	600	20	23.21	3.21	134.11
3	700	20	23.74	3.74	156.25
4	800	20	24.28	4.28	178.82
5	900	20	24.81	4.81	200.96
Average			**23.742**	**3.742**	**156.33**

It is observed from these that as the mass flow rate of water through solar FPC increases from 0.001 kg/s to 0.01 kg/s the average heat gain by the water remains almost constant at 156.30 but outlet water temperature rise decreases from 37.35°C to 3.742°C.

4.1.1 Effect on solar flat plate collector temperature contours

Temperature contours of solar flat plate collector for five mass flow rates i.e. 0.001 kg/s to 0.01 kg/s are shown in Figure 4.1 to 4.5 respectively.

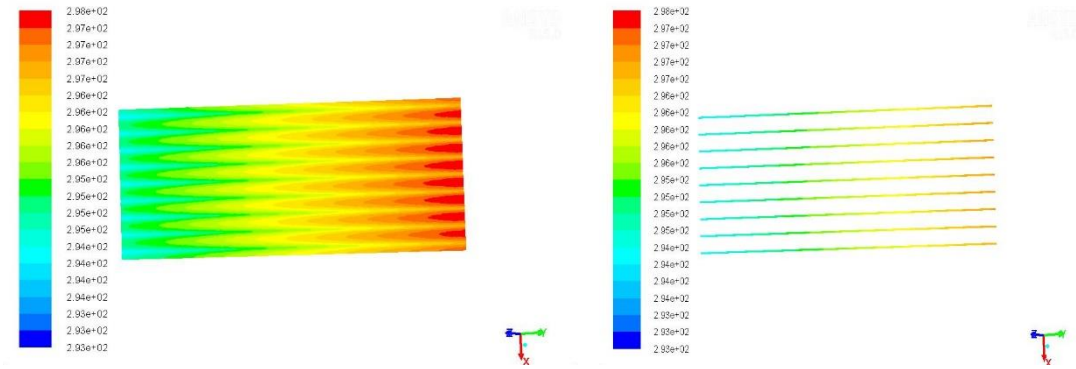

Fig. 4.1: Temperature contours of Solar FPC at m_f = 0.001 kg/s

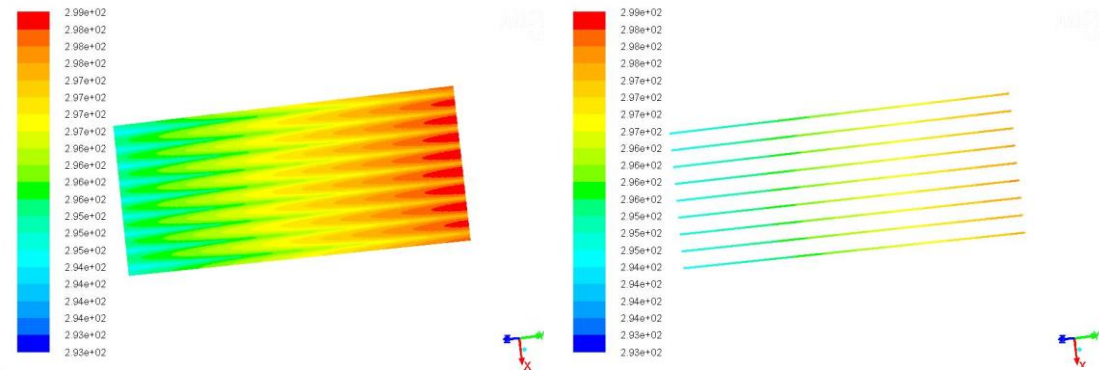

Fig. 4.2: Temperature contours of Solar FPC at m_f = 0.0025 kg/s

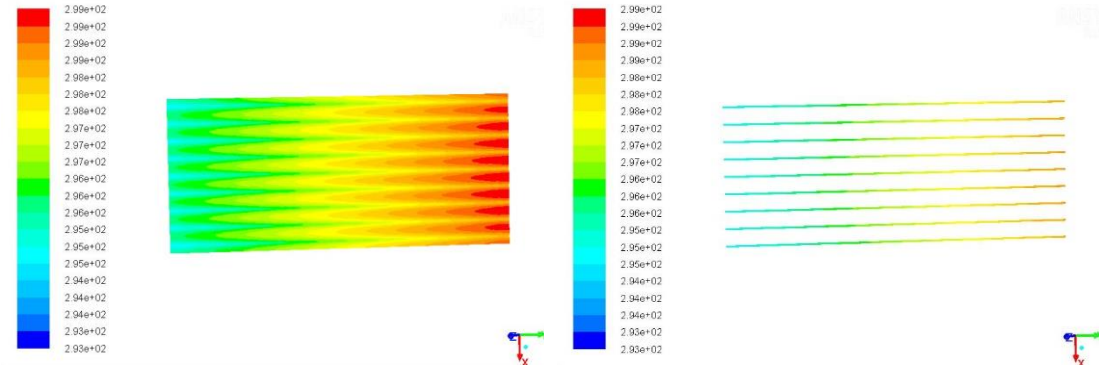

Fig. 4.3: Temperature contours of Solar FPC at m_f = 0.005 kg/s

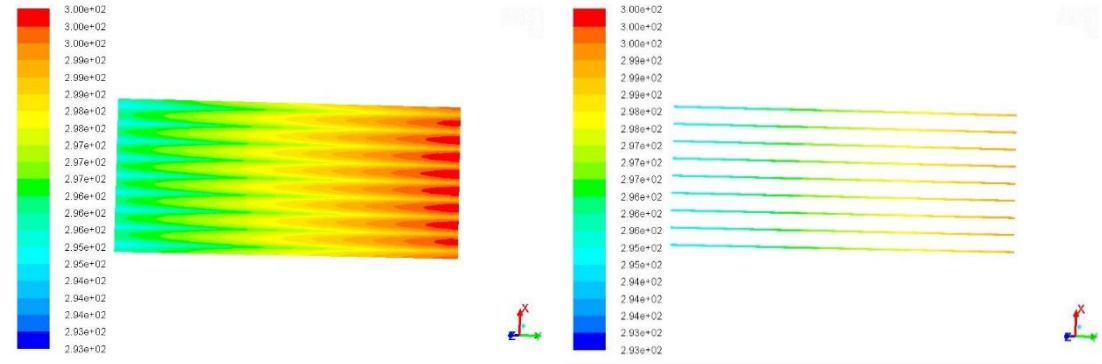

Fig. 4.4: Temperature contours of Solar FPC at m_f = 0.0075 kg/s

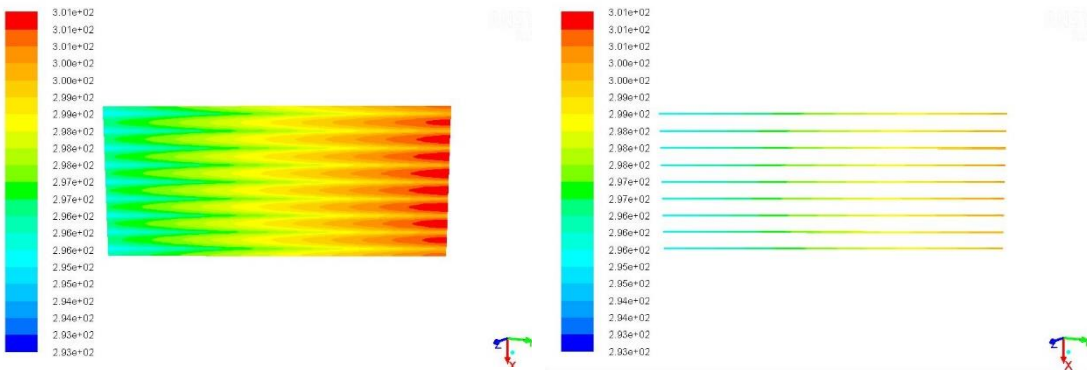

Fig. 4.5: Temperature contours of Solar FPC at m_f = 0.01 kg/s

It is clear from these figures that as the mass flow rate of water through solar FPC increases from 0.001 kg/s to 0.01 kg/s the outlet water temperature decreases. It is important to note that in the application of solar FPC increase in mass flow rate of water decreases its outlet temperature and low outlet temperature is not useful in many applications. So, in order to get the maximum outlet temperature, mass flow rate should be as low as possible.

4.2Effect of mass flow rate on performance of STHX

Different mass flow rates ranging from 60 kg/hr to 180 kg/hr have been considered for CFD simulation to study the effect of shell side and tube side mass flow rate on the performance of shell and tube heat exchanger. Other parameters such as shell fluid inlet and tube fluid inlet are taken same in all cases. Effectiveness of heat exchanger and outlet temperatures are calculated from CFD results and are shown below in table 4.6 to 4.8.

Table 4.6: simulated results for outlet temperature at m_{sf1} = 60 kg/hr

Temperature at zones (°C)	Mass Flow rate of tube side fluid		
	$\dot{m}_{tf1}$ = 60 kg/hr	$\dot{m}_{tf2}$ = 120 kg/hr	$\dot{m}_{tf3}$ = 180 kg/hr
Shell fluid inlet	20	20	20
Shell fluid outlet	44.37	41.40	39.83
Tube fluid inlet	85	85	85
Tube fluid outlet	60.51	62.52	65.53

Table 4.7: simulated results for outlet temperature at m_{tf1} = 120 kg/hr

Temperature at zones (°C)	Mass Flow rate of tube side fluid		
	$\dot{m}_{tf1}$ = 60 kg/hr	$\dot{m}_{tf2}$ = 120 kg/hr	$\dot{m}_{tf3}$ = 180 kg/hr
Shell fluid inlet	20	20	20
Shell fluid outlet	42.53	40.38	39.12
Tube fluid inlet	85	85	85
Tube fluid outlet	57.96	59.65	61.15

Table 4.8: simulated results for outlet temperature at m_{tf1} = 180 kg/hr

Temperature at zones (°C)	Mass Flow rate of tube side fluid		
	$\dot{m}_{tf1}$ = 60 kg/hr	$\dot{m}_{tf2}$ = 120 kg/hr	$\dot{m}_{tf3}$ = 180 kg/hr
Shell fluid inlet	20	20	20
Shell fluid outlet	40.23	39.02	37.09
Tube fluid inlet	85	85	85
Tube fluid outlet	53.67	55.31	57.42

It is observed from these tables that performance of shell and tube heat exchanger depends on both shell side and tube side heat exchanger. Increase in shell side mass flow rate with keeping tube side flow rate as constant decreases the outlet temperature of both shell and tube fluid, and increase in tube side mass flow rate with keeping shell side flow rate as constant also have the same trend as with shell side. Since decrease in flow rate provides much time for heat transfer between fluids thus better heat transfer can be achieved. So, in order to achieve high heat transfer flow rates must be low for both the side.

4.2.1 Effect on solar flat plate collector temperature contours

Temperature contours of shell and tube heat exchanger for different shell and tube side flow rates i.e. 60 kg/hr to 180 kg/hr are shown in Figure 4.6 and 4.7 respectively.

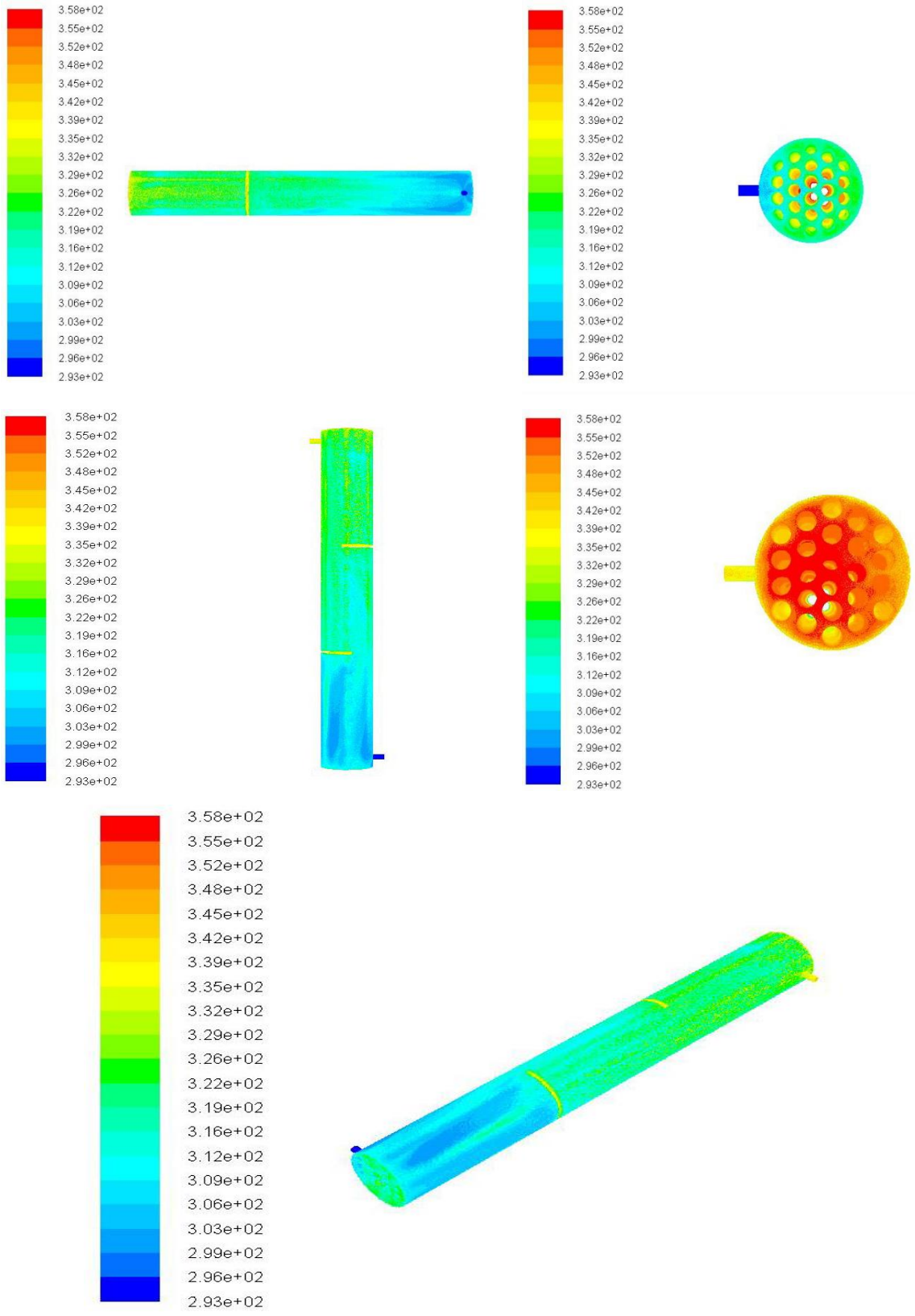

Fig. 4.6: Temperature contours of shell fluid of shell and tube heat exchanger.

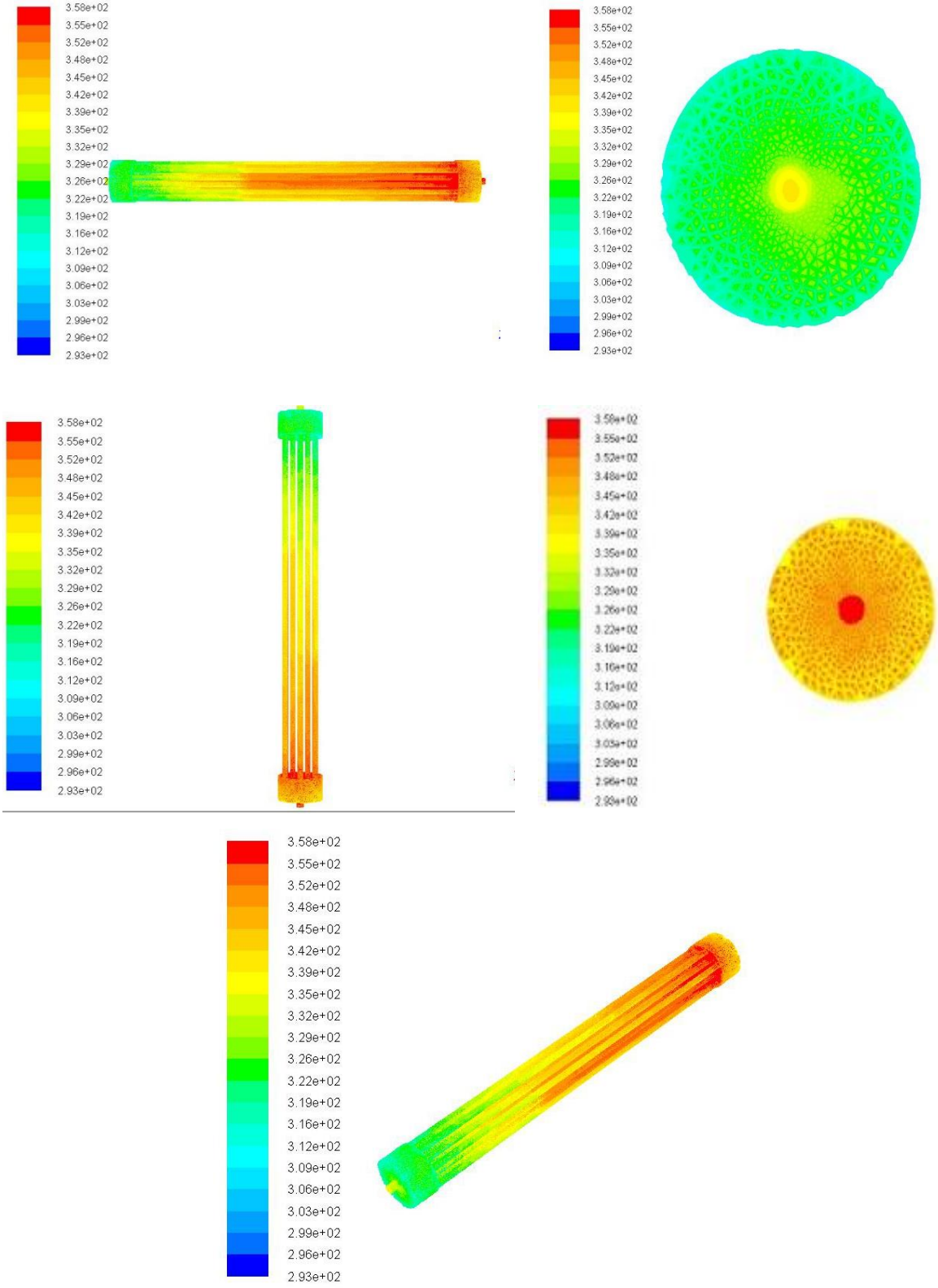

Fig. 4.7: Temperature contours of tube fluid of shell and tube heat exchanger.

Temperature contours of shell and tube heat exchanger shows the temperature distributions within the shell and tube heat exchanger. Hot fluid is flowing inside the

tubes and cold fluid is flowing through the shell. Very good variation of temperature can be seen within the shell and tube heat exchanger with the help of temperature contours.

Chapter 5

Results and Discussions

The geometric modelling (unstructured mesh) of solar flat plate collector and shell and tube heat exchanger was performed using SOLIDWORKS and CFD analysis were carried out using FLUENT. Parametric and performance study was carried out to optimize the performance of solar FPC and STHX. In this study three-dimensional, steady state model of solar FPC and STHX has been developed by employing energy equation and standard k-ε turbulence model and analysed. The CFD simulation results were compared and validated with experimental results.

In this simulation study, solar flat plate collector was simulated in order to get optimum performance. Mass flow rate of water is optimised and other parameters were kept constant. The optimised mass flow rate in order to achieve the maximum outlet temperature through the solar flat plate collector is 0.001 kg/s. During the optimization, different mass flow rates ranging from 0.01 kg/s to 0.001 kg/s have been considered for CFD simulation.

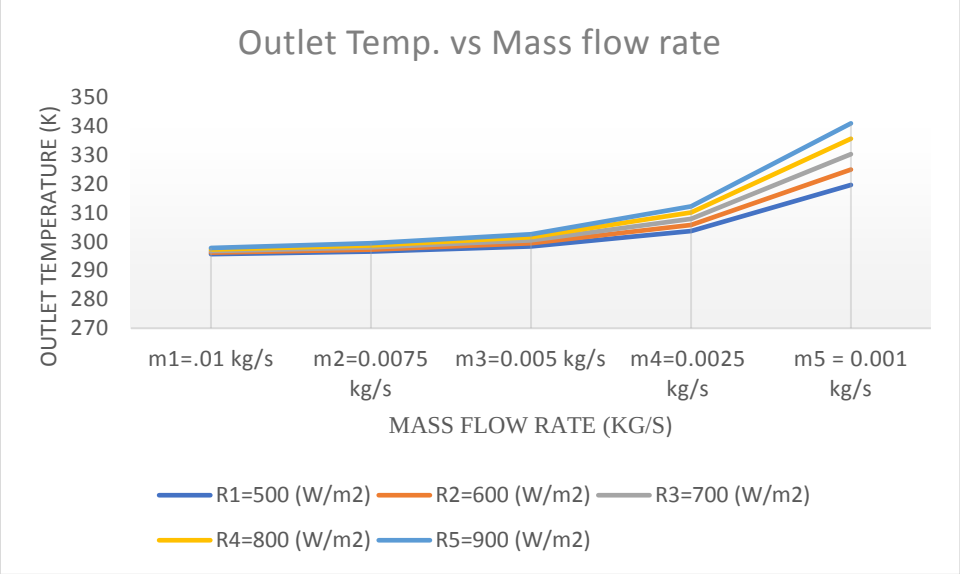

Fig. 5.1: variation in outlet temperature with mass flow rate.

It can be clearly concluded from Figure 5.1 that at maximum outlet temperature is achieved at mass flow rate of 0.001 kg/s. Decrease in mass flow rate increases the outlet

temperature through the solar flat plate collector, so natural convection flow provides better results compared to forced flow.

5.1 Optimised performance of shell and tube heat exchanger

In this simulation study, shell side mass flow rate and tube side mass flow rate are optimised and other parameters are kept constant. By optimising the mass flow rate of shell and tube side fluid the overall performance of shell and tube heat exchanger has been enhanced. It is observed from these tables that performance of shell and tube heat exchanger depends on both shell side and tube side mass flow rates. Increase in shell side mass flow rate with keeping tube side flow rate as constant decreases the outlet temperature of both shell and tube fluid, and increase in tube side mass flow rate with keeping shell side flow rate as constant also have the same trend as with shell side.

Effectiveness has been calculated on the basis of simulated results and at different mass flow rates, different effectiveness values are given below in table 5.1.

Table 5.1: Effectiveness calculated from simulation results for different mass flow rates

	$\dot{m}_{tf1}$ = 60 kg/hr	$\dot{m}_{tf2}$ = 120 kg/hr	$\dot{m}_{tf3}$ = 180 kg/hr
$\dot{m}_{sf1}$ = 60 kg/hr	0.39	0.32	0.30
$\dot{m}_{sf2}$ = 120 kg/hr	0.41	0.39	0.32
$\dot{m}_{sf3}$ = 180 kg/hr	0.45	0.42	0.36

From the table 5.1 it can be clearly seen that shell and tube heat exchanger with configuration of tube side mass flow rate ($\dot{m}_{tf}$) as 60 kg/hr and shell side mass flow rate ($\dot{m}_{sf}$) as 180 kg/hr gives the best effectiveness.

Chapter 6

Conclusion

A detailed literature survey was carried out to study the work performed by different researchers in the field of solar flat plate collector and shell and tube heat exchanger considering different aspects of solar thermal energy conversion system such as mass flow rate of shell fluid, mass flow rate of tube fluid and fluid flow rate in solar FPC significantly. Some researchers tried different approach to find the optimum performance of shell and tube heat exchanger like effect of mass flow rate on overall heat transfer coefficient, overall heat transfer through the system and introduction of baffles etc. and showed better thermal performance than conventional types.

Initially two shell and tube heat exchangers with same dimensions and different tube configurations were modelled and analysed using CFD in order to get the optimum tube configuration for parametric analysis. Shell and tube heat exchanger was designed, modelled and simulated using CFD technique. Geometrical modelling of solar flat plate collector and shell and tube heat exchanger was carried out in SOLIDWORKS. Grid generation (unstructured grid) and defining the types of boundaries for the system were carried out in ANSYS software. Using FLUENT version 6.3 software, parametric and performance study was carried out to optimize the shell and tube heat exchanger. For this purpose, a three-dimensional, steady state model of staggered tube arrangement shell and tube heat exchanger has been developed by employing energy equation and standard k-ε turbulence model and analysed.

Experimental results of a shell and tube heat exchanger with same configurations were observed and results of numerical simulations were validated by the experimental results. Comparison of the CFD simulation results with experimental results shows good agreement and thus the developed model was validated.

This valid CFD model has been used for the parametric study of solar flat plate collector and shell and tube heat exchanger. Mass flow rate has been considered as a parameter that could affect the performance of both solar flat plate collector and shell and tube heat exchanger.

It is observed during the simulation process that for optimum performance of solar flat plate collector, mass flow rate of fluid must be very low (in this study 0.001 kg/s flow rate of water is considered as the lowest flow rate) so that time available for heat transfer will be more and thus outlet temperature of fluid will be more. For shell and tube heat exchanger, it is observed that performance of shell and tube heat exchanger depends on both shell side and tube side mass flow rates. Increase in shell side mass flow rate with keeping tube side flow rate as constant decreases the outlet temperature of both shell and tube fluid, and increase in tube side mass flow rate with keeping shell side flow rate as constant also have the same trend as with shell side. The best configuration of mass flow rate for optimum performance of shell and tube heat exchanger is 60 kg/hr and 180 kg/hr for tube side and shell side mass flow rates respectively.

➢ Scope for future work

Following recommendations are proposed for future work:

- Geometric analysis can be done on existing model of shell and tube heat exchanger and based on the results of analysis, modifications can be done.
- Other operating parameters such as number of baffles, baffles spacing, number of tube can be optimised for further research.
- This study was performed for steady state, so in future for further research transient state can also be considered.
- Natural convection provides the best results for solar flat plate collector, but for accurate analysis surrounding temperature, wind velocity and other such parameters can also be analysed.
- This CFD study can be done with finer mesh size nearer to inlets and outlets of solar flat plate collector and shell and tube heat exchanger for better results.

References

1. A. F. Jozaei, A. Baheri, M. K. Hafshejani, A. Arad (2012), "Optimization of baffle spacing on heat transfer, pressure drop and estimated price in a shell and tube heat exchanger" World Applied Sciences Journal, 18, 1727-1736.
2. A. Singh, S. S. Sehgal (2013), "Thermo-hydraulic analysis of shell and tube heat exchanger with segmental baffles" ISRN Chemical Engineering, Vol. 2013.
3. A. A. Bakhtiari, A. Hematian, Y. Ajabsirchi, (2012), "Experimental analysis of flat plate solar air collector efficiency" Indian Journal of Science and Technology, 5, 3183-3187.
4. A. L. H. Costa, E. M. Queiroz, (2008), "Design optimization of shell and tube heat exchangers", Applied Thermal Engineering, 28, 1798-1805.
5. A. S. Ambekar, R. Sivakumar, N. Anantharaman, M. Vivekenandan (2016), "CFD simulation study of shell and tube heat exchangers with different baffle segment configurations", Applied Thermal Engineering, 108, 999-1007.
6. A. Mathur, G. D. Agrawal, M. Chandel (2012), "Recent development in the field of solar water heater using flat plate collector: A review" International Journal of Advanced Engineering Technology, 3, 68-70.
7. A. A. Bhuiyan, A. K. M. Sadrul Islam, (2016), "Thermal and hydraulic performance of finned tube heat exchangers under different flow ranges: A review on modelling and experiment" International Journal of Heat and Mass Transfer, 101, 38-59.
8. A. Alimoradi, (2017), "Study of thermal effectiveness and its relation with NTU in shell and helically coiled tube heat exchanger" Case Studies in Thermal Engineering, 9, 100-107.
9. B. T. Lebele-Alawa, V. Egwanwo (2012), "Numerical analysis of the heat transfer in heat exchangers" International Journal of Applied Science and Technology, 2, 60-64.
10. D. S. Patel, R. R. Parmar, V. M. Prajapati, (2015), "CFD analysis of shell and tube heat exchangers – A review" International Research Journal of Engineering and Technology, 2, 2231-2235.
11. D. J. Bhatt, P. M. Jhavar, P. J. Sakariya, (2014), "International Journal for Scientific Research & Development, 2, 446-453.

12. D. Rai, S. Bharati, S. Bux (2015), "To study the parametric analysis of shell and tube heat exchanger" IJRAIIE, 1, 383-391.
13. E. Pal, I. Kumar, J. B. Joshi, N. K. Maheshwari (2016), "CFD simulation of shell side flow in a shell and tube type heat exchanger with and without baffles", Chemical Engineering Science, 143, 314-340.
14. G. P. Yadav, K. K. Khan, (2016), "Experimental investigation of helical baffles shell and tube heat exchanger using Aluminum Oxide (II) nanoparticle", International Journal of Interdisciplinary Research, 2, 527-531.
15. G. Y. Zhou, L. Y. Zhu, H. Zhu, S. T. Tu, J. J. Lei, (2014), "Prediction of temperature distribution in shell and tube heat exchangers" 6th International Conference on Applied Energy – ICAE2014, 61, 799-802.
16. H. Shokouhmand, M. R. Salimpour, M. A. Akhavan-Behabadi, (2008), "Experimental investigation of shell and coiled tube heat exchangers using Wilson plots" International communication in Heat and Mass Transfer, 35, 84-92.
17. H. Li, V. Kottke, (1997), "Effect of baffle spacing on pressure drop and local heat transfer in shell and tube heat exchangers for staggered tube arrangement", International Journal of Heat and Mass Transfer, 41, 1303-1311.
18. I. Tari, E. Ozden, (2010), "Shell side CFD analysis of a small shell and tube heat exchanger", Energy Conversion and Management, 51, 1004-1014.
19. I. A. Badruddin, S. M. Shahril, G. A. Quadir, N. A. M. Amin, (2017), "Thermo-hydraulic performance analysis of shell and double concentric tube heat exchanger using CFD", International Journal of Heat and Mass Transfer, 105, 781-798.
20. J. P. Garcia, R. H. Martin, A. G. Pinar, (2011), "Experimental heat transfer research in enhanced flat plate solar collectors", World Renewable Energy Congress – Sweden, 3844-3851.
21. J. Wen, S. Wang, Y. Li, (2009), "An experimental investigation of heat transfer enhancement for a shell and tube heat exchanger", Applied Thermal Engineering, 29, 2433-2438.
22. J. Yang, L. Ma, J. Bock, A. M. Jacobi, W. Liu, (2014), "A comparison of four numerical modelling approaches for enhanced shell and tube heat exchangers with experimental validation", Applied Thermal Engineering, 65, 369-383.

23. Jeomer. C. S., S. Thomas, Rakesh D., Nidheesh P., (2015), "Optimization of shell and tube heat exchanger by baffle inclination and baffle cut", International Journal of Innovative Research in Science, Engineering and Technology, 4, 69-73.
24. K. Anand, V. K. Pravin, P. H. Veena, (2014), "Experimental investigation of shell and tube heat exchanger using bell Delaware method", International Journal for Research in Applied Science and Engineering Technology, 2, 73-85.
25. K. Uzuneanu, A. Teodoru, T. Panait, J. J. G. Martins, (2014), "Optimum tilt angle for solar collectors with low concentration ratio", Advances in Fluid Mechanics and Heat & Mass Transfer, 2, 123-128.
26. L. Zhang, Y. Xia, B. Jiang, X. Xiao, X. Yang, (2013), "Pilot experiment study on shell and tube heat exchangers with small angles helical baffles", Chemical Engineering and Processing, 69, 112-118.
27. M. Saffarian, T. Yousefi, M. K. Moraveji, (2014), "Numerical analysis of shell and tube heat exchanger with simple baffle by CFD", International Journal of Science and Research, 7,1334-1345.
28. P. R. Prasad, H. V. Byregowda, P. B. Gangavati, (2010), "Experimental analysis of flat plate collector and comparison of performance with tracking collector", International Journal for Research in Applied Science and Engineering Technology, 1, 63-75.
29. P. Ranjitha, V. Somashekar, A. B. Jamuna, (2013), "Numerical analysis of solar flat plate collector for circular pipe configuration by using CFD", International Journal of Engineering Research and Technology, 2, 3356-3362.
30. Q. W. Wang, B. Peng, C. Zhang, (2007), "An experimental study of shell and tube heat exchangers with continuous helical baffles", Journal of Heat Transfer, 129, 1425-1431.
31. S. Ramasamy, P. Balashanmugam, (2015), "Thermal performance analysis of the solar water heater with circular and rectangular absorber fins", International Journal of Innovative Science, Engineering and Technology, 2, 596-603.
32. S. Wang, J. Wen, H. Yang, Y. Xue, X. Tong, (2015), "Experimental investigation on performance comparison for shell and tube heat exchangers with different baffles", International Journal of Heat and Mass Transfer, 84, 990-997.
33. S. A. Kalogiru, (2004), "Solar thermal collectors and applications", Progress in Energy and Combustion Science, 30, 231-295.

34. V. K. Patel, R. V. Rao, (2010), "Design optimization of shell and tube heat exchanger using particle swarm optimization technique", Applied Thermal Engineering, 30, 1417-1425.
35. V. V. Kumar, B. Jayachandriah, (2015), "Design of helical baffle in shell and tube heat exchanger and comparing with segmental baffles using kern method", International Journal of Emerging Technology in Computer Science and Electronics, 13, 157-162.
36. V. Chalwa, N. Kadli, (2013), "Study of variation for pressure drop and temperature distribution in a shell and tube heat exchanger in case of vertical baffle", Mechanica confab, 2, 17-25.
37. Y. Wang, Z. Liu, S. Huang, W. Liu, W. Li, (2011), "Experimental investigation of shell and tube heat exchanger with a new type of baffles", Heat and Mass Transfer, 47, 833-839.
38. Y. You, Y. Chen, M. Xie, X. Luo, L. Jiao, S. Huang, (2015), "Numerical simulation and performance investment for a small size shell and tube heat exchanger with trefoil-hole baffles.

Appendix A-1

i. Navier Stokes equations

$$\nabla = \bar{i}\frac{\partial}{\partial x} + \bar{j}\frac{\partial}{\partial y} + \bar{k}\frac{\partial}{\partial z}$$

∇ is del or nabla operator

$$div(\vec{F}) = \frac{\partial u}{\partial x} + \frac{\partial v}{\partial y} + \frac{\partial w}{\partial z}$$

div is divergence of a vector

ii. Continuity equation

$$\frac{\partial \rho}{\partial t} + \nabla.(\rho\vec{v}) = S_m$$

ρ is density in kg/m^3, $\vec{v}$ is the velocity vector in m/s, S_m is the source term for mass generation in kg/m^3, t is the time in seconds.

iii. Momentum equation

$$\frac{\partial}{\partial t}(\rho\vec{v}) + \nabla.(\rho\vec{v}\vec{v}) = -\nabla p + \rho\vec{g} + \vec{F}$$

p is the static pressure in Pa, $\vec{g}$ is the gravitational body force, $\vec{F}$ external body forces in N/m^3 and $\vec{F}$ also contains other model-dependent source terms such as porous media and heat source sources.

iv. The energy equation

$$\frac{\partial}{\partial t}(\rho E) + \nabla.(\vec{v}(\rho E + p)) = \nabla.[k_{eff}\nabla T - \sum_j (h_j \vec{J}_j + (\tau_{eff}.\vec{v}))] + S_h$$

Where, k_{eff} is the effective conductivity (k + k_t, where k_t is turbulent conductivity), $\vec{J}_j$ is the diffusion flux of species j. the first three terms on the right-hand side represent transfer due to conduction, species diffusion and

various dissipation respectively. S_h includes the heat of chemical reaction and any other volumetric heat sources.

v. Turbulent model

$$\frac{\partial}{\partial t}(\rho k)+\frac{\partial}{\partial x_i}(\rho k \mu_i)=\frac{\partial}{\partial x_i}(\alpha_k \mu_{eff}.\frac{\partial k}{\partial x_i})+G_k+G_b-\rho\varepsilon-Y_m+S_k$$

and

$$\frac{\partial}{\partial t}(\rho\varepsilon)+\frac{\partial}{\partial x_i}(\rho\varepsilon\mu_i)=\frac{\partial}{\partial x_i}(\alpha_\varepsilon \mu_{eff}.\frac{\partial \varepsilon}{\partial x_j})+C_{1\varepsilon}\frac{\varepsilon}{k}(G_k+C_{3\varepsilon}G_b)-C_{2\varepsilon}\rho\frac{\varepsilon^2}{k}-R_\varepsilon+S_k$$

In these equations, G_k represents generation of turbulence kinetic energy due to the mean velocity gradients, G_b is the generation of turbulence kinetic energy due to buoyancy, Y_m represents the fluctuating dilation in compressible turbulence to the overall dissipation rate. The quantities α_k and α_ε are the inverse effective Prandtl numbers for k and ε, respectively. S_k and S_ε are user defined source terms.

Publications

- Karan Yadav, Vikash Gora, Mohan Jagadeesh Kumar Mandapati, (2017), "Numerical Simulation of shell and tube heat exchanger with and without baffles", International Journal of Engineering and Advanced Technology, 6, 62-65.